IDOWU OSELUMHE ILEKURA

ESTIMATING WAVE RUNUP USING SATELLITE MULTI-SPECTRAL IMAGERY

UNIVERSIDADE DO ALGARVE

Faculdade de Ciências e Tecnologia

2024

IDOWU OSELUMHE ILEKURA

ESTIMATING WAVE RUNUP USING SATELLITE MULTI-SPECTRAL IMAGERY

Master's in Coastal Hazards, Risks, Climate Change Impacts and Adaptation

Performed under the supervision of:
Luis Pedro Almeida
Professor Óscar Manuel Ferreira

UNIVERSIDADE DO ALGARVE

Faculdade de Ciências e Tecnologia

2024

ESTIMATING WAVE RUNUP USING SATELLITE MULTI-SPECTRAL IMAGERY

Declaration of authorship of work

I hereby declare to be the author of this work, which is original and unpublished. Authors and works consulted are properly cited in the text and included in the reference list.

(Idowu Oselumhe Ilekura)

ACKNOWLEDGEMENTS:

I want to begin by appreciating my main supervisor, Luis Pedro Almeida, who supported me throughout the thesis work, without whose support I would not have been able to accomplish the thesis. His assistance before embarking on the thesis when I drafted my dissertation plan, during the data collection process and analysis, the interpretation of the results, and the writing review process, was instrumental to the project's success. I also thank him for always coming to my aid whenever I faced difficulties in all areas while undergoing the thesis work and for providing a safe haven during the thesis report. He was exceptionally calm and thoughtful when explaining and answering all my technical and non-technical questions that I have.

I must also appreciate my other supervisor, Professor Óscar Manuel Ferreira, and my thesis advisor, Catarina Marques Cecilio, for their support during the thesis writing and for providing valuable criticism that helped perfect my writing. Especially Professor Óscar Manuel Ferreira for the suggestions and ways to improve the writing, backed by his years of experience in the coastal space.

My thanks to the CoastHazar consortium, who selected me two years ago to embark on the amazing journey of studying coastal hazards and proffering solutions to climate-related issues. Without the selection, I would not have considered working on my thesis project, which was amazing. I also appreciate the lecturers and professors who selflessly imparted their years of experience in the industry and academia to help grow our knowledge.

I will not fail to appreciate the support of my CoastHazar colleagues during the master's program, especially Yusuf Taofiq Damilola, Syeda Arooba Shah, Mayowa Basit Adbulsalam, Muhammad Naeem, Clenmar Rowe and Lavanya Hemanath.

On a personal note, I would like to thank my mother, Ilekura-Iyasele Grace Udegua and my siblings, Monica Ibeh, Omolola Lawal, Kehinde Ilekura, and Taiwo Ilekura, for their emotional support throughout the thesis period and for always having a listening ear to all the challenges I faced during the course of my master's degree. Also, to my spiritual family, Deeper Life Bible Church, Den Haag, Netherlands, I am grateful for the spiritual, emotional, and all-around

support during my stay in the Netherlands and for making it easy to integrate into the Netherlands.

Finally, I would like to express my appreciation to myself for persevering and staying focused throughout the two-year master's program. I am grateful to God through my Lord Jesus Christ for the grace and fortitude to go through my master's program and complete my thesis in peace. To my friend Goodness Onyinyechi Ekaba, thanks for the emotional support throughout the thesis and master's program.

ABSTRACT

The wave runup is one of the most important processes responsible for coastal hazards, including overtopping or erosion. Understanding and predicting wave runup in any coastal environment is crucial for risk and vulnerability assessment studies. Nevertheless, the lack of field observations of wave runup is one of the main limitations of the predictability of this process. Past studies have used shore-based video monitoring techniques to observe wave runup in coastal areas. However, these studies were limited in time (data acquisition periods of several months or years) and space (spatial coverage of a single beach or extension of hundreds of meters or a few kilometres). In recent years, remote sensing, in particular Satellite Imagery, have improved the capability of the onboard sensor (e.g., improved spatial resolution of optical sensors) and revisit times (time between consecutive data collection in the same point on the earth's surface), making of this technology one with the most significant potential to overcome earth sciences challenges. The present project's general objective is to utilize multi-spectral imagery to monitor wave runup in coastal areas, representing a novel approach compared to past runup monitoring methodologies. Wetsand (boundary between the dry and wet beach) and Waterline (boundary between the water and the beach) were extracted from the satellite images as potential runup proxies. The satellite-derived runup proxies were compared to existing wave runup formulations. The error quantification was performed using statistical descriptive parameters (e.g., RMSE, correlation coefficient, and Bias). The waterline-derived runup proxies demonstrated high correlation (Bias = 0.35, R^2 = 0.63, RMSE = 0.65) with the existing runup formulation, whereas the Wetsand proxies exhibited lower correlation (Bias = -0.41, R^2 = 0.17, RMSE = 0.95). Averaging the Wetsand and Waterline proxies improved the Bias and RMSE to 0.12 and 0.611, respectively. The optimal formulation for each proxy was employed to correct the runup formulation, which was then used to compute the R_2, resulting in a refined runup formulation. The corrected formulations for each proxy were utilized to predict extreme runup events. The waterline and the average Wetsand/Waterline proxies outperformed the Wetsand proxies during low wave and tide conditions. In contrast, the Wetsand proxy outperformed both alternatives in predicting extreme runup under high wave and tide conditions. Overall, the study noted the prospect of using satellites to measure and estimate runup globally.

RESUMO

O espraio induzido pelas ondas é um dos processos mais importantes responsáveis pelos perigos em zonas costeiras, incluindo o galgamento e a erosão. Compreender e prever o espraio induzido pelas ondas em qualquer ambiente costeiro é crucial para estudos de avaliação de risco e vulnerabilidade. No entanto, a falta de observações de campo do espraioé uma das principais limitações da previsibilidade deste processo. Estudos anteriores utilizaram técnicas de monitorização com base em vídeo-monitorização para observar o espraio em zonas costeiras. No entanto, esses estudos foram limitados no tempo (períodos de aquisição de dados de vários meses ou anos) e no espaço (cobertura espacial de uma única praia).
Nos últimos anos, a deteção remota, em particular o uso de imagens de satélite, melhorou a capacidade dos sensores a bordo (por exemplo, melhoria da resolução espacial dos sensores ópticos) e os tempos de revisita (tempo entre coletas de dados consecutivas no mesmo ponto da superfície da Terra), tornando esta tecnologia uma das mais promissoras para superar os desafios das ciências da Terra. O objetivo geral do presente trabalho é utilizar imagens multiespectrais para monitorizar o espraio induzido pelas ondas em zonas costeiras, representando uma abordagem inovadora em comparação com metodologias passadas de monitorização do espraio.
Para concretizar o objetivo, foram descarregadas imagens de satélite da missão Planetscope e da missão Sentinel-2.. A linha seco-molhado (a fronteira entre a praia seca e molhada) e a linha de água instantânea (a fronteira entre a água e a praia) foram delineadas no QGIS e extraídas das imagens de satélite como possíveis indicadores do espraio. As posições horizontais da linha de água e da linha do seco-molhado foram convertidas para elevação vertical com perfis topográficos atualizados e descarregados a partir do portal web do Programa de Monitorização Costeira de Portugal Continental (COSMO).
Os indicadores de espraio derivados de satélite foram comparados com formulações de espraio de ondas existentes, incluindo Holman (1986), Stockdon et al. (2006), e Vousdoukas et al. (2012). A quantificação do erro foi realizada utilizando parâmetros estatísticos descritivos (por exemplo, RMSE, coeficiente de correlação e Bias). Os proxies derivados da linha de água demonstraram uma correlação mais alta (Bias = 0,35, R^2 = 0,63, RMSE = 0,65) com a formulação de espraio existente, enquanto os proxies da linha de seco-molhado exibiram menor correlação (Bias = -0,41, R^2 = 0,17, RMSE = 0,95). A elevada correlação entre o espraio e linha de água foi atribuída ao facto de a linha de água capturada no momento da aquisição da imagem, estar altamente correlacionada com as condições das ondas no

momento da aquisição da imagem. Já a linha de seco-molhado pode estar relacionada a um evento de ondas que ocorreu horas antes do momento da aquisição da imagem, e por esse motivo as correlações serem mais baixas. As formulações corrigidas para cada indicador de epsraio foram utilizadas para prever o espraio durante um evento extremo, para avaliar o desempenho das formulações corrigidas em eventos extremos. O evento extremo foi a tempestade Hércules, que ocorreu entre 5 e 7 de janeiro de 2014, causando danos ao longo da costa portuguesa. Os indicadores da linha de água e a média da linha de seco-molhado superaram os proxies da linha de humidade durante condições de ondas e marés baixas. Em contraste, o proxy da linha de humidade superou ambas as alternativas na previsão de runup extremo sob condições de ondas e marés altas. A linha d'água e a média da linha de humidade/linha d'água mostraram ser melhores indicadores de runup para prever o runup extremo sob condições mínimas, e a linha de humidade para condições extremas máximas. O estudo mostrou que, embora a medição e estimativa do espraio com satélites seja nova, a possibilidade de medir e estimar o espraio é viável globalmente. No entanto, para estender a abordagem para uma nova área de estudo, é necessário ter disponíveis certos parâmetros. Estes incluem parâmetros consistentes de boias de ondas locais que capturam os processos locais, perfis abundantes e morfologicamente mutáveis para converter a extensão horizontal para vertical, e uma plataforma de imagens de satélite com pouca ou nenhuma cobertura de nuvens, o que pode melhorar o número de imagens descarregadas. Além disso, os indicadores de espraio serão validados com medições de espraio de campo da área de estudo

TABLE OF CONTENTS

ACKNOWLEDGEMENTS: iv
ABSTRACT vi
RESUMO vii
LIST OF FIGURES: xi
LIST OF TABLES: xiii
LIST OF ABBBREVATIONS. xiv
1.0 INTRODUCTION: 1
1.1 Motivation 1
1.2. Research Objectives: 4
1.2.1 General 4
1.2.2 Specific 4
1.3 Research Questions 4
1.4 Thesis Structure 4
2.0 LITERATURE REVIEW 6
2.1 Wave Runup Processes 6
2.2 Runup Measurements 6
2.3 Runup Estimation Methodology 7
2.3.1 Estimating Runup with Wave Parameters 8
2.3.2 Estimating Runup with Wave Parameters and Beach Morphology 8
2.4 Conclusion 10
3.0 STUDY AREA 11
3.1 Location 11
3.2 Geomorphology 11
3.3 Waves and Tide Dynamics 12
3.4 Region of Interest 13
4.0 METHODOLOGY 15
4.1 Datasets 15
4.1.1 Topographic data – beach profiles 15
4.1.2 Satellite Imagery 15
4.2 Data Processing 17
4.2.1 Satellite Image Horizontal Displacement Assessment 17
4.2.2 Waterline and Wetsand Mapping 17
4.2.3 Converting Waterline/ Wetsand Horizontal Positions to Vertical Elevations 18
4.3 Data Analysis 19

4.3.1 Wave and Tidal Data Exploratory Analysis 19
4.3.2 Beach Slope Computation 19
4.3.3 Effect of Topographic Changes on Runup Proxies 20
4.3.4 Satellite-derived runup formulation. 22
4.3.5 Assessment of Satellite-derived runup equation during an extreme event 22
5.0 RESULT 23
5.1 Wave and Tide Parameters Analysis 23
5.2 Beach Morphology Effect on Runup Proxies 23
5.3 Runup Analysis 26
5.3.1 Comparison of Runup Equations with Runup Proxies 26
5.3.2 Choosing and correcting the best Runup Formulation for each proxy 29
5.3.3 Assessing the Satellite-derived runup formulation for each proxy on Predicting Extreme Events 30
6.0 DISCUSSION 32
6.1 Runup Indicators 32
6.1.1 Wetsand and Waterline as Runup Indicators 32
6.1.2 Average Wetsand/ Waterline as Indicator 33
6.2 Effect of Morphology/ Topography on Wave Runup 35
6.3 Application of Satellite-Derived Runup Formulations 36
7.0 Conclusion / Recommendations 37
7.1 Challenges Faced 37
7.2 Future Work/ Recommendations 38

LIST OF FIGURES:

Figure 1: Total Water at the Coast (adapted from Lowe, 2021) 1

Figure 2: Exemplification of Runup and Setup Processes (source: CoastalWiki) 3

Figure 3: Difference in Resolution between Sentinel-2 and Planetscope, with the indication of the position of the instantaneous waterline (dashed blue line; adapted from Doherty et al., 2022) 3

Figure 4: Runup Timestack Image obtained from Video Cameras (Stockdon et al., 2006). The runup peaks can be seen from the image. 7

Figure 5: Case Study Map. (a) Subaerial image of Costa Da Caparica, with the sand banks. (b) The location of Costa Da Caparica in Portugal. (c) The expanded view of Costa Da Caprica. 13

Figure 6: Selected Region of Interest and the Survey Transect for all downloaded profiles are shown in red. 14

Figure 7: Profiles Downloaded from COSMOS with Distance from the Dune and Elevation. The green, red, blue, and black lines correspond to profiles downloaded in December 2018, December 2019, January 2021 and May 2021, respectively. 16

Figure 8: Calendar of the extracted satellite images, with days when images were downloaded. Days when Sentinel-2 images were downloaded are circled in red, and when Planet Scope images were downloaded are circled in Blue. 17

Figure 9: The Waterline and Wetsand delineation process: The Waterline is shown in red, and Wetsand in blue. The Waterline is between the minimum white and maximum brownish pixel, and Wetsand is between the minimum deep brownish pixel and the maximum less brownish pixel. 18

Figure 10: Waterline, Wetsand Horizontal to Vertical conversion of Image 2021-05-05 using May-05-2021 profile 19

Figure 11: Beach Slope Computation: The Maximum Wetsand elevation, maximum Wetsand distance, minimum Waterline elevation, and minimum Waterline distance are shown in blue, green, red, and black, respectively. 20

Figure 12: Timeseries plot of Wave and Tide Parameters. Subplots (A-D) are for the Wave height (HS), Peak period (TP), Wave direction and Tide level. The dashed green line indicates the image acquisition days. 23

Figure 13: Effect of Beach Morphology on Runup Proxies Horizontal Extent conversion to Vertical elevation. Subplot A and B shows the time series plot between proxy elevation obtained with different profiles shown in blue and proxy elevation obtained with 2018 profile (same profile) shown in green for Wetsand and Waterline respectively. Subplot B and D shows the histogram distribution plot between proxy elevation obtained with different profiles shown in red and proxy elevation obtained with 2018 profile (same profile) shown in blue. 25

Figure 14: Wetsand Elevation comparison with runup formulations. Subplot A-C shows the timeseries comparison between Wetsand elevation and predicted $R2$ for Stockdon et al. (2006), Holman (1986) and Voudouskas et al. (2012). Subplot D-F shows the scatter plot between the

Wetsand elevation and predicted $\boldsymbol{R2}$ for Stockdon et al. (2006), Holman (1986) and Voudouskas et al. (2012). 27

Figure 15: Waterline Elevation comparison with runup formulations. Subplot A-C shows the timeseries comparison between Waterline elevation and predicted $\boldsymbol{R2}$ for Stockdon et al. (2006), Holman (1986) and Voudouskas et al. (2012). Subplot D-F shows the scatter plot between the Wetsand elevation and predicted $\boldsymbol{R2}$ for Stockdon et al. (2006), Holman (1986) and Voudouskas et al. (2012). 27

Figure 16: Average Wetsand/Waterline elevation comparison with runup formulations. Subplot A-C shows the timeseries comparison between Average Wetsand/Waterline elevation and predicted $\boldsymbol{R2}$ for Stockdon et al. (2006), Holman (1986) and Voudouskas et al. (2012). Subplot D-F shows the scatter plot between the Average Wetsand/Waterline elevation and the predicted $\boldsymbol{R2}$ for Stockdon et al. (2006), Holman (1986) and Voudouskas et al. (2012). 28

Figure 17: Assessment of the Maximum Hercule's Storm Runup Prediction Level at Costa da Caparica. The maximum runup value indicated in dashed green corresponds to the highest values of all runup proxy formulation predictions. 31

Figure 18: Wave collision instance at Costa da Caparica. Source 31

Figure 19: Hercule's storm runup prediction values for all runup proxy formulation on the beach. The beach profile corresponds to the 2018 survey profile, and the maximum and minimum values correspond to the maximum and minimum values of the wave and tide during the storm period. 35

LIST OF TABLES:

Table 1: Extracted Survey Profiles from COSMOS with Profile Name and the Date the survey was conducted. 14

Table 2: Sentinel-2 and PlanetScope Image Properties 16

Table 3: Wave and Tide Parameters during Hercules Storm 22

Table 4: Statistical metrics of Runup proxies' horizontal extent to vertical elevation for waterline and Wetsand using different profiles and same profiles (2018) 25

Table 5: Runup Proxy comparison with Runup Formulation Statistics. 28

Table 6: Runup Proxies formulation performance on predicting Hercule's storm Runup. $R2$_min and $R2$_max correspond to the runup level for the minimum and maximum wave and tide parameters during the storm period. 30

Table 7: Statistical Metrics comparison for the best runup proxy formulation 34

LIST OF ABBBREVATIONS.

HS – Significant Wave Height
H – Wave Height
TP – Peak Period
RMSE – Root Mean Squared Error
QGIS - Quantum Geographic Information System
Dir – Wave Direction
SDR- Satellite-Derived Runup
MSI – Multi-Spectral Imagery
EO – Earth Observation
R_2 – Wave Runup exceeded by 2% of the total runup measured.
ξ - Surf Similarity or Iribarren Number
ξ_0 – Surf Similarity computed with offshore parameters.
L_0 – Wavelength measured in offshore conditions
H_0 – Wave Height measured in offshore conditions.
R^2 – R-squared.
$<\eta>$ - Setup
S- Swash
S_{inc} – Incident Swash
S_{IG} – Infragravity Swash

1.0 INTRODUCTION:

1.1 Motivation

On open coasts, wave-induced runup is the most important component, contributing to the most extreme sea levels and one of the primary mechanisms responsible for coastal overtopping, flooding, and erosion (Hoeke et al., 2013; Melet et al., 2016, 2018; Almar et al., 2021).

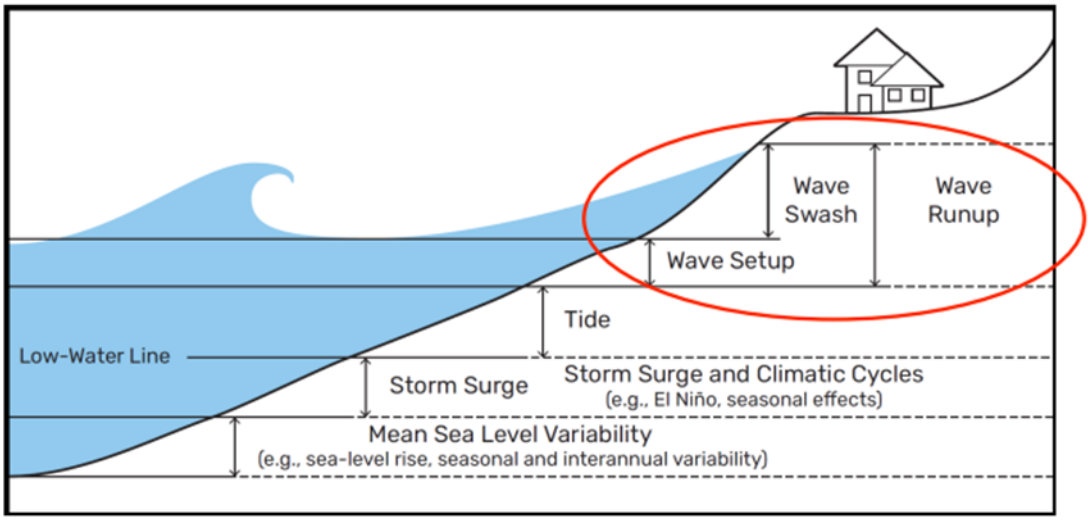

Figure 1: Total Water at the Coast (adapted from Lowe, 2021)

Wave runup can be defined as the maximum vertical extent of wave uprush on a beach or structure above the still water level. Wave runup results from a combination of two wave-induced processes: the wave setup and the swash component (Holman & Guza, 1984). The wave setup is caused by the breaking of waves that release energy as momentum flux, popularly referred to as radiation stress (Longuet-Higgins & Stewart, 1964) .The release of momentum causes a depression at the surf zone (wave setdown) and an elevation at the coast (setup) to counterbalance the gradient difference (Figure 2). At the same time, the swash occurs due to undispersed momentum in the breaking wave, which reaches the shore with a bore and oscillates around the setup (Stockdon et al. 2006; Gomes Da Silva et al. 2020) .Wave runup is influenced by several factors, including wave height, wave period, beach slope, type of beach (e.g., dissipative or reflective) and (or) the presence of natural or artificial structures or obstacles on the beach profile.

The wave runup determines how much flooding and erosion occur on the coast; therefore, it is a crucial variable to estimate. Several authors have developed empirical equations to predict the wave runup on natural beaches. Stockdon et al. (2006) developed some of the most widely

used empirical runup formulas based on a comprehensive analysis of video-derived runup time series from various sandy beaches. Their research incorporated deep-water wave and tide information, as well as local beach profile topography. Although the formulas developed by Stockdon et al. (2006) were based on numerous observations, they were limited to sandy beaches and specific ranges of wave and tidal conditions. Consequently, the applicability of these formulas is restricted, potentially limiting their accuracy and effectiveness in different coastal environments with varying sediment types, wave exposures, and tidal ranges. This limitation underscores the need for further research and data collection across a broader spectrum of coastal settings to develop more versatile and comprehensive empirical runup formulas (Gomes da Silva et al., 2020). One of the primary limitations to enhancing existing empirical formulas for wave runup is the insufficient number of observations from diverse coastal environments. Variations in wave exposure, tidal ranges, and sediment compositions significantly influence runup, yet data from these different contexts are scarce. This scarcity is largely because most runup datasets have been collected using shore-based local video-monitoring systems. While effective for detailed studies at specific locations, this approach is constrained by its limited spatial scope and difficulty in replication across broader regional or global scales. Expanding data collection to include a wider variety of coastal environments through advanced monitoring technologies, such as satellite Earth Observations (EO), can be explored to address this challenge. The EO sensors, including passive methods that acquire multi-spectral satellite images, have global coverage, with a temporal resolution that can range from 1 to 5 days (for the cases of PlanetScope and Sentinel 2, respectively) and spatial resolutions from 3 up to 10 m, represent a candidate to address this challenge. Despite the relatively low temporal resolution (several days, compared with hourly runup observations performed with video-monitoring techniques) and moderate spatial resolution, satellite imagery has global coverage and historical datasets that offer a unique opportunity to assess the wave runup at any coastal region. It is crucial to highlight that the traditional methodological approach for estimating runup from video-imagery primarily involves conducting statistical analyses on short burst of images (e.g., 15-minute long) at the start of every hour. These images are captured at very high temporal resolutions, typically around 4Hz, and are collected hourly. This method allows for detailed assessment of tidal influences and rapid changes in the offshore wave climate. However, when assessing the possibility to use EO imagery as an additional source of data to study wave runup, the temporal resolution is significantly lower, typically restricted to daily observations at best. Consequently, employing the same methodological approach becomes impractical. Therefore, assessing EO imagery for runup analysis requires

first a preliminary assessment and possibly a distinct methodology tailored to its unique data characteristics.

The recent advances in the spatial and temporal resolution of new satellite missions, such as Sentinel 2 and PlanetScope, have improved the detection of the instantaneous waterline used in shoreline studies (Almeida et al., 2021; Doherty et al., 2022) , a proxy that has the potential to be used as a proxy of wave runup (e.g., instantaneous waterline or wet/dry line) (Figure 3).

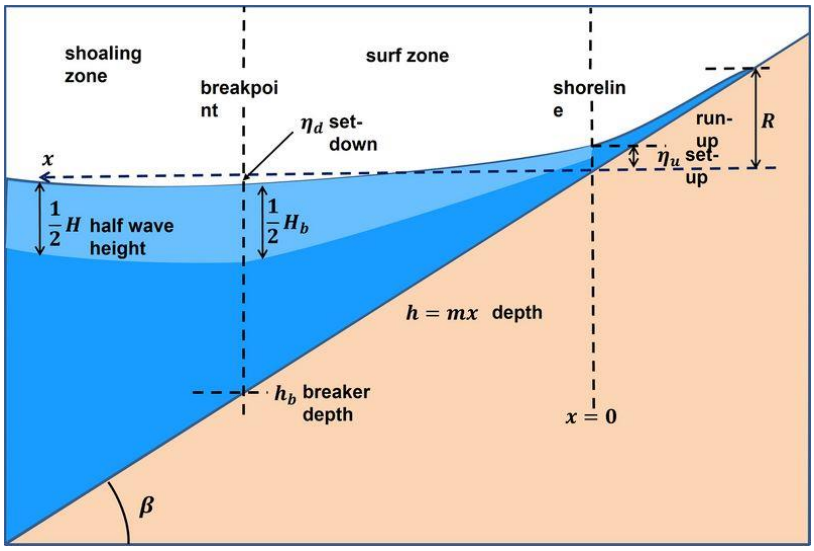

Figure 2: Exemplification of Runup and Setup Processes (source: CoastalWiki)

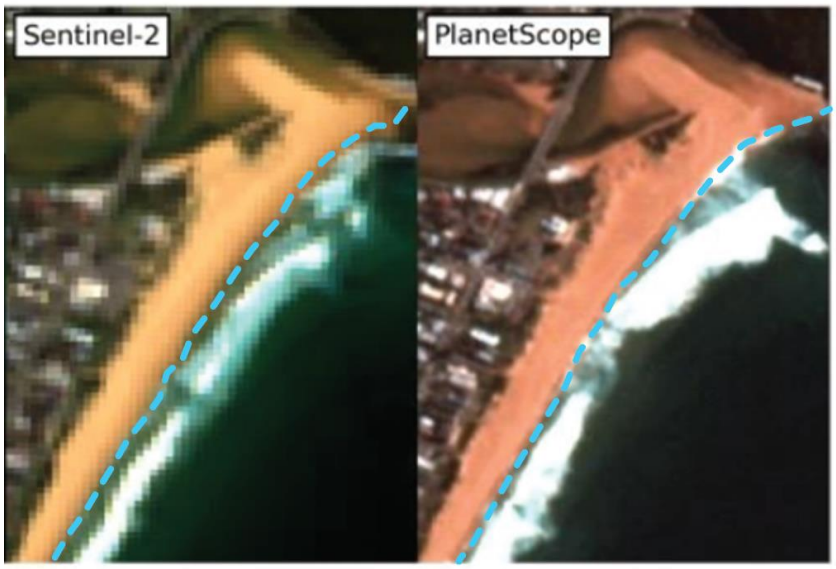

Figure 3: Difference in Resolution between Sentinel-2 and Planetscope, with the indication of the position of the instantaneous waterline (dashed blue line; adapted from Doherty et al., 2022)

The present project aims to evaluate the use of EO imagery (Sentinel 2 and PlanetScope) to estimate wave runup on coastal sandy beach (Caparica beach, located on the central west coast

of Portugal), using has auxiliary data in-situ morphology (beach profile topography, to convert x,y waterline positions into z elevations). The analysis will focus on historical datasets and the relationship between the main forcing mechanisms of wave runup, including waves, astronomical and meteorological tides, coastal morphology (slope) and satellite-derived runup (SDR) elevation at coincident times, using a similar approach implemented in the past using video-imagery (e.g., Stockdon et al., 2006). Due to the lack of in-situ wave runup observations at the study site, the comparison between estimated SDR will be performed against estimations using existing empirical equations and error quantification analysis will be performed using traditional statistical indicators (root mean squared error, correlation coefficient and bias).

1.2. Research Objectives:

1.2.1 General

- Develop a new methodological approach to derive wave runup from satellite imagery and quantify the associated errors.

1.2.2 Specific

I. Digitize runup indicators (instantaneous waterline and wet/dry positions) from historical satellite images from two missions manually: Sentinel-2 and PlanetScope

II. Compare the time-series of satellite-derived runup indicators with runup estimations (using empirical formulas) and quantify the differences

1.3 Research Questions

The research questions that the study aims to answer are:

1. Can satellite imagery observe wave runup in coastal areas?
2. How important is coastal morphology for runup estimation?
3. Can we use SDR to predict storm impact in coastal areas?

1.4 Thesis Structure

Six chapters—Introduction, Literature Review, Methodology, Results, Discussion, and Conclusion—have been used to structure the thesis flow.

a) The introduction chapter will introduce the thesis project, its relevance, challenges with past work, the thesis objectives, and the research questions the thesis aims to answer.

b) The Literature Review section will review the state-of-the-art approach to measuring and estimating runup formulations. It will start by exploring the processes contributing to wave runup at the coast and how past authors have measured, estimated, and formulated wave runup formulations. It will analyze the shortcomings and conclude that a new approach is needed to measure runup with satellite images.
c) The methodology section will outline the steps for measuring and estimating wave runups with satellite images. It will start with data gathering, processing the extracted images, and analysis.
d) The results section will present the findings in the data analysis section of the methodology. The result will be presented in charts or figures, tables and text.
e) The discussion section will discuss insights from the data analysis section and use research papers to provide technical and sound arguments.
f) The conclusion will identify the key points from the discussion section, draw a conclusion from the discussion, identify the challenges faced, and provide recommendations to improve the work.

2.0 LITERATURE REVIEW

2.1 Wave Runup Processes

As waves approach the coast, they undergo several transformations, including shoaling and eventually breaking. Waves carry momentum flux, and when they break, this momentum is released. The release of momentum flux results in a depression in the surf zone and an elevation of the water level along the coast, known as set-up, which balances out the elevation gradient caused by set-down (Longuet-Higgins & Stewart, 1964). Wave breaking also generates an uprush of water onto the coast due to the energy released. This uprush causes an increase in water level at the shoreline, known as run-up, which depends on the characteristics of the swash zone. (Holman & Guza, 1984) defined wave runup as the maximum vertical extent of uprush on the shoreline relative to still-water level, encompassing both set-up (elevation due to wave breaking) and swash (backwash and uprush motion of water).

2.2 Runup Measurements

The early works measuring runup were performed on physical laboratory environments and wave flumes where natural waves propagating, breaking and runup were reproduced over beach profiles. The tools used for measuring the runup included a capacitor-induced transducer, which translates the wetness due to runup into the distance, as (Synolakis, 1987) used. The main challenge with laboratory experiments is the difficulty of capturing all the morphodynamics and morphology that occurs on natural beaches, which has a higher level of complexity that these preliminary experiments were capable of reproducing. In addition, the difficulty of scaling grain size for laboratory experiments is a significant challenge (Bayle et al., 2021). Following these initial physical modelling studies, wave runup research was driven by initial field observation experiments. Initial field experiments were developed by Guza & Thornton (1982), who used resistance wires to measure runup. After these initial experiments, wave runup observations were performed with land-based remote sensing using a video-monitoring technique.

The measurement of runup from video cameras involves placing a video camera that faces the longshore position of the beach and taking a video record of the runup at specific time intervals, such as 10 min bursts every hour (approach developed by Vousdoukas et al., (2012)). During the recording, a single cross-section of pixels is selected (timestack), from which temporal wave runup information is extracted Fig. 4.

Based on these observations, the runup timeseries is generated by relating the elevation of the beach profile topography to the water line position measured along the pixel time stack. Thus, the initial horizontal runup information is converted into vertical runup.

Runup is often used to analyze the accuracy of coastline extraction from satellite imagery; (Cabezas-Rabadán et al., 2020) used runup estimation to validate the extracted coastline in Faro Beach. The validation process used the intersection between the beach profile and the total water level, which involves the runup to mark the beach shoreline. The beach shoreline through the intersection was compared with the extracted satellite coastline. However, to our knowledge, no method exists to define runup from satellite imagery.

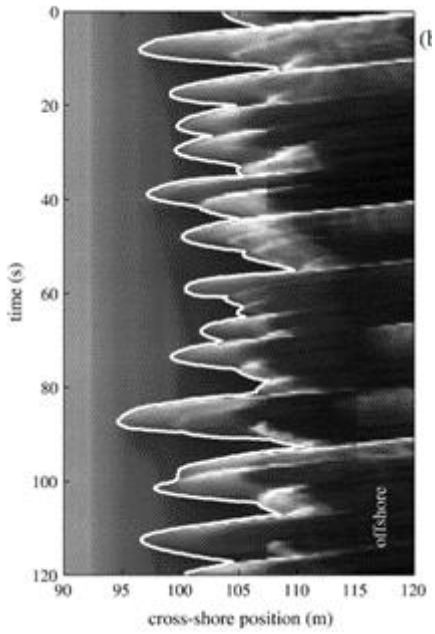

Figure 4: Runup Timestack Image obtained from Video Cameras (Stockdon et al., 2006). The runup peaks can be seen from the image.

2.3 Runup Estimation Methodology

The Estimating runup is mainly done by developing an empirical formulation that depends on finding relationships between runup observations and wave and tide parameters of beach morphology.

2.3.1 Estimating Runup with Wave Parameters

Early work on estimating the runup was done with the offshore wave height. Authors such as (Miche (1951), cited by (Gomes da Silva et al., 2020), found a linear relationship between the wave runup and the offshore wave height. However, Miche (1951) also found that the linear relationship ceases to exist even with increased wave height because of the energy saturation. The assumption made by Miche was also confirmed by Synolakis (1987), who experimented in the laboratory and found the relationship between the offshore wave height scaled with the depth of the wave flume with the runup, as shown in Equation 1.

$$\frac{R}{d} = 1.109\left(\frac{H}{d}\right)^{0.582} \quad (1)$$

Where R is the runup, H is the wave height, and d is the depth of the water.

2.3.2 Estimating Runup with Wave Parameters and Beach Morphology

When waves travel from deep water towards the coast, the interactions with the beach morphology, such as slope and reduced depth, lead to the wave properties' transformation. Hence, the beach morphology properties should be accounted for while estimating runup. The Irribarren number or the surf similarity parameter ξ captures the beach slope and wave parameters such as wave height and length; several authors have tried to use this parameter to estimate runup.

To estimate the runup of waves that break on solid coastal structures, Hunt (1959) found a correlation between the runup on the structures and the slope captured in the Irribarren number. The correlation led Hunt (1959) to propose the first equation that relates the runup with the Irribarren number and the wave height, as shown in Equation 2.

$$\frac{R}{H} = K\xi \quad (2)$$

The formula proposed by Hunt, (1959) was further extended by Holman (1986) who used video techniques to measure runup in collaboration with the Field Research Facility (FRF) at Duck, North Carolina. Holman, (1986) extracted 154 runup values, on further analysis, it was found that the runup scaled with the offshore wave height correlated better with the surf similarity computed with the offshore wave parameters (ξ_0) The observation led to the derivation of an empirical formulation, as shown in Equation 3

$$\frac{R_2}{H_S} = (0.83\xi_o + 0.2) \quad (3)$$

Where R_2 is the runup surpassed by 2% of all the runup values and signifies the extreme runup. ξ_0 is the offshore irribarean or surf similarity computed with offshore wave parameters.

The equation is commonly called the Holman runup equation and can be used to determine runup at different beaches. However, a notable limitation of the Holman (1986) equation is its lack of general applicability. Given that the equation was derived from data at a single beach location, its applicability to diverse beach environments may be limited.

To solve the problem of generalisation of the Holman runup formula, Stockdon et al., (2006) decided to extend The Holman formular for different beaches and different conditions. The extension was done, by collecting 10 videos recorded runup data from the Netherlands and the USA, with beach having ξ_0 that varies between 0.07 and 3.25 which indicates dissipative, intermediate and reflective. The two hypotheses were that the R_2 is the sum of the setup $<\eta>$ and half of the swash as shown in equation (4), and secondly that the swash is made up of the square root of the addition of the square of incident and infragravity swash as shown in equation (5)

$$R_2 = <\eta> + \frac{S}{2} \tag{4}$$

$$S = \sqrt{(S_{inc})^2 + (S_{IG})^2} \tag{5}$$

The two hypotheses were tested on dissipative with $\xi_0 < 0.3$ and reflective beaches with $\xi_0 > 0.3$. The foreshore slope had less impact on the runup on dissipative beaches, while it played a significant role on reflective beaches. The observation led to two distinct runup formulations for dissipative and reflective beaches, as shown in Equation (6) and Equation (7)

$$R_2 = 0.043(H_0 L_0)^{\frac{1}{2}} \tag{6}$$

$$R_2 = 0.73\beta_f(H_0 L_0)^{\frac{1}{2}} \tag{7}$$

While considering both the dissipative and reflective beaches, the general form of runup equation was derived as shown in Equation (8)

$$R_2 = 1.1\left(0.35\beta_f(H_0 L_0)^{\frac{1}{2}} + \frac{[H_0 L_0(0.563\beta_f^2 + 0.004)]^{\frac{1}{2}}}{2}\right) \tag{8}$$

The Stockdon et al, (2006) equation is one of the most used methods for computing runup, given that it combines several parameters.

2.4 Conclusion

The literature review reveals that previous authors have attempted to quantify and predict wave runup through various methods, including laboratory experiments, field measurements, video analysis, and statistical modelling. However, a significant challenge in past studies has been the limited temporal scope of the experiments, which often span only a few days. This can make it challenging to capture extreme runup events.

Considering these limitations, this thesis addresses the aforementioned challenges by leveraging multi-spectral images spanning years to decades to measure and estimate runup.

3.0 STUDY AREA

3.1 Location

The study site selected for the present work is located in the central west coast of Portugal, in the north section of Caparica coastal stretch, near the Tagus estuary mouth in the Almada municipality (geographical location: latitude 38.56 degrees North and longitude -9.1936 West). This section of the coast is characterized by a low-lying sandy topography, with a beach face (average beach width of approximately 50 to 100 m) backed by low dune ridge. Inland from the frontal dune ridge is a densely urbanized area, reason why this dune ridge has a crucial role in protecting inland human occupation.

3.2 Geomorphology

The Caparica beach is an exposed sandy beach with a shoreline characterized by an arch and a low-lying dune that extends to the south of the selected study site (Pereira et al., 2022). The coastal plain of Caparica is primarily composed of alluvial sediment composed of fine and coarse sand from the Tagus River with average sediment size which ranges from 0.2 mm to 0.7mm with a predominate size of 0.3 mm (Sancho, 2023). The north part of Caparica Beach is characterized by the presence of a low dune ridge that has been subject to some interventions in the past for stabilization. The central section of Caparica beach has undergone structural erosion problems, and for that reason has been subject to interventions, and is characterized by the presence of a seawall which leads to beach encroachment. The coast of Caparica beach is significantly affected by anthropogenic activities such as dredging (in Tagus estuary main channel), sand nourishment interventions (Veloso-Gomes et al., 2009; Pereira et al., 2022; Silva et al., 2013). The Caparica lost approximately 1.8 million m^3 of sediment in the northward area between September 2001 and July 2007 at an average rate of 310000 m^3/ year (Silva et al., 2013). However, between the interval of July 2007 to May 2010, the lost sediment was recovered at a rate of 640000 m^3/ year (Silva et al., 2013) due to sand nourishment intervention. These values illustrate the important morphological and volumetric variability that this coastal stretch presents over time.

According to Ponte Lira et al. (2016), which have analysed shoreline position from 1958 to 2010, this coastal area is under significant erosion, with an average rate change of about -4.57 ± 0.2 m year-1. According to the same author the shoreline rates of changes present an important

spatial variability, with the north section demonstrating a more erosive behavior while the southern portion presenting accretion.

The structural erosion problems identified in the north section of Caparica beach led to the introduction of groins, several beach nourishment projects, seawalls, and revetments to stabilise the coastline and control erosion rate (Veloso-Gomes et al., 2009). The Cachopo Norte sand banks flank Costa da Caparica to the south and the Cachopo Sul sand bank to the North, the sand banks have been subjected to morphological changes over the years (Fortunato et al., 2021). The sand banks play a key role in dissipating waves by breaking and limiting the wave height at Costa da Caparica (Fortunato et al., 2021).

3.3 Waves and Tide Dynamics

Caparica Beach is oriented from north to northwest and is highly exposed to Atlantic waves, which predominantly arriving towards the coast from the north-west direction. According to Costa et al. (2001), energetic waves predominantly occur during the winter months (from October to March), with significant wave heights (Hs) greater than 5 metres.

Caparica beach has a North-North and North-West orientation and highly exposed to Atlantic waves that originate predominantly from the north-west. According to Costa et al. (2001), energetic waves predominantly occur during the winter months (October to March), with significant wave heights (Hs) greater than 5 metres.

To characterise the wave information at Costa da Caparica, Raposeiro et al. (2013) analysed wave information from the Port of Lisbon wave buoy between 30-12-2005 and 16-11-2012. The Hs ranges from 0.27 to 6.19 m, with an average of 1.22 m. The wave peak period (Tp) ranged from 1.9 to 28.6 s, with a mean of 10.8 s. The wave direction varies from north to south , with an average from west and common interval of between west and north-west. The results of the author's analysis indicated that Caparica Beach experiences energetic waves, with a high wave period, predominantly originating from the north-western direction. Other authors, such as Palma et al. (2021), have also observed that the predominant wave direction for the beach is from the northwest. The northwestern waves suffer an important refraction process at the Targus entry, resulting in the rotation of waves as they approach the coast, modifying their angle of attack to the north instead of their original incident angle from northwest (Palma et al. 2021)

The high exposure to energetic wave conditions at Costa da Caparica has resulted in extreme coastal hazards, including wave overtopping and erosion at the beach. Garzon et al. (2020) analysed wave events from 2000 to 2019. The authors identified 26 extreme events, representing 74% of the time with extreme events. Nevertheless, the authors also discovered that energetic waves occur more frequently during winter and less during summer.

Caparica has been described by several authors as a mesotidal area with a semi-diurnal tidal curve, with a maximum high tide level of 1.95 m and a spring tide amplitude of approximately 3.8 m (Veloso-Gomes et al., 2009). However, meteorological tidal values have been observed to reach up to 0.5m, with the occurrence of storm surges (Veloso-Gomes et al., 2009).

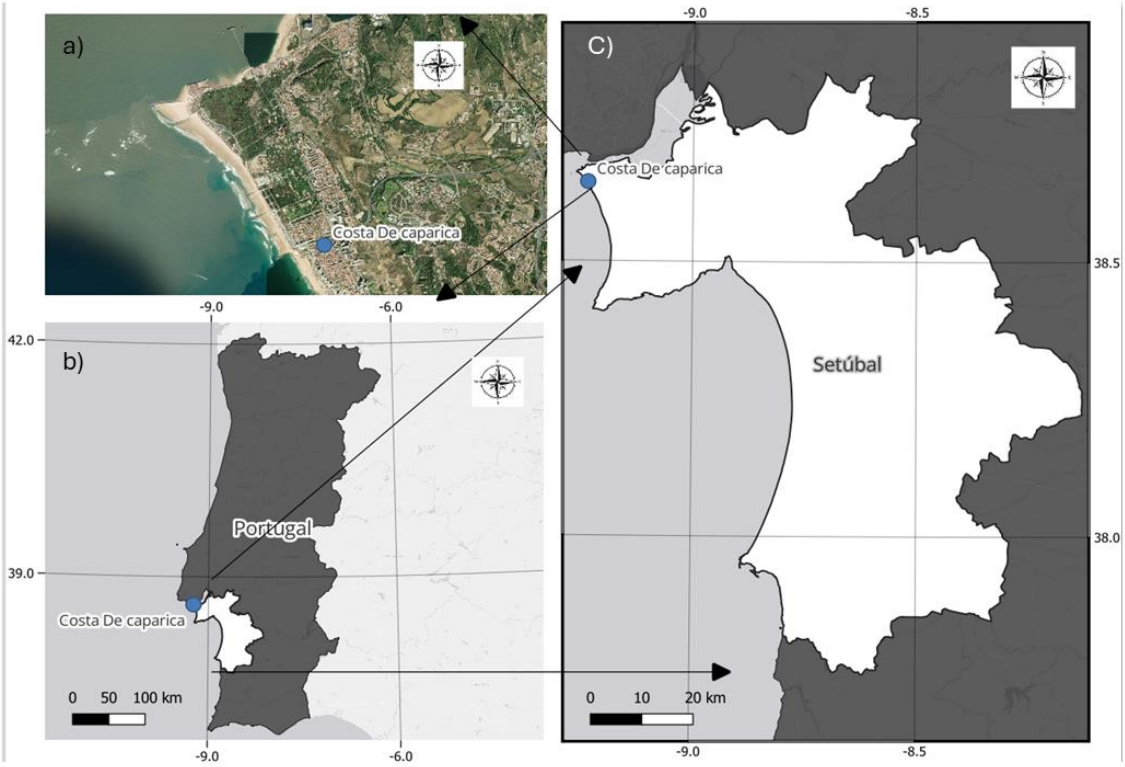

Figure 5: Case Study Map. (a) Subaerial image of Costa Da Caparica, with the sand banks. (b) The location of Costa Da Caparica in Portugal. (c) The expanded view of Costa Da Caprica.

3.4 Region of Interest

The region of interest selected for the present work is a cross-section of Caparica beach located in the Sao Joao da Caparica beach, as shown in Figure 6. The area shares characteristics similar to those of the rest of the north sector of Caparica Beach. The region was selected because it coincided with the location of the Coastal Monitoring Programme of Continental Portugal

(COSMO) survey. COSMOS is responsible for surveying beach profiles in Portuguese Coastal areas. In the present work the topobathymetric survey data from COSMO was used (profile code P06) The beach profiles were measured with GPS-RTK along several cross-shore sections within the domain of the study areas over different periods of the year. The vertical datum of the beach profiles is the mean sea level (zero is equal to the mean water elevation measured by the Cascais tide gauge). This morphological data was surveyed with GPS-RTK (subaerial part) and single beam echosounder (subtidal part) over different periods of the year (Table 1). The vertical datum of the beach profiles is the mean sea level (zero is equal to the mean water elevation measured by the Cascais tide gauge). This survey data provided valuable information on the vertical changes that took place between 2018 and 2021, including the beach nourishment intervention carried out in November 2019.

Table 1: Extracted Survey Profiles from COSMOS with Profile Name and the Date the survey was conducted.

Profile Names	Date of Survey
PT_PO6_20181227	2018-12-27
PT_PO6_20191230	2019-12-30
PT_PO6_20210701	2021-07-01
PT_PO6_20210506	2021-05-06

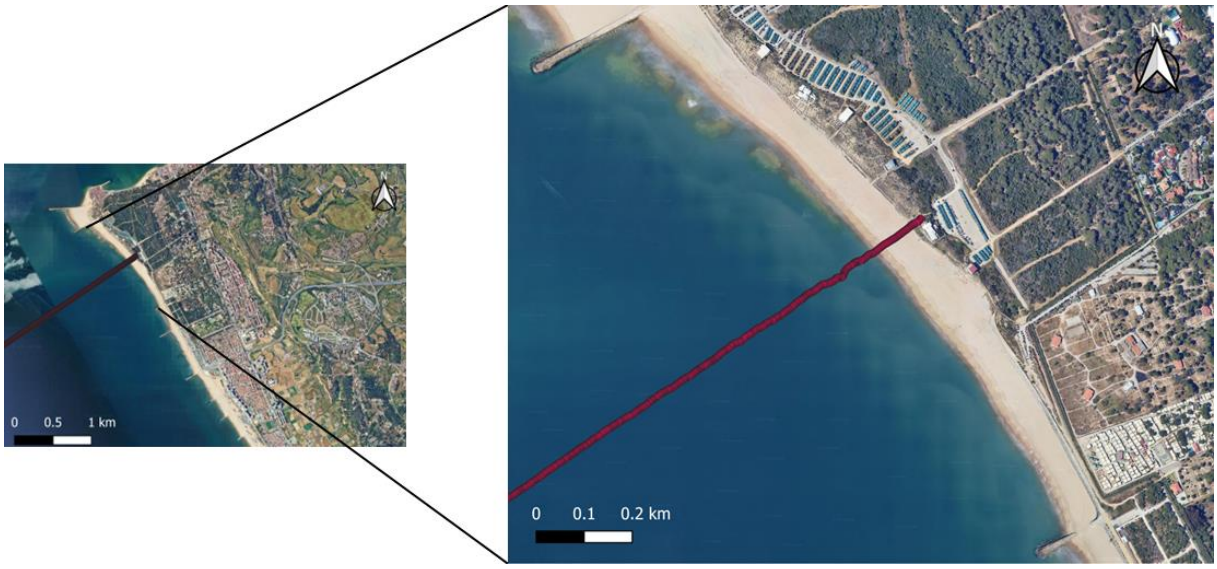

Figure 6: Selected Region of Interest and the Survey Transect for all downloaded profiles are shown in red.

4.0 METHODOLOGY

4.1 Datasets

4.1.1 Topographic data – beach profiles

In order to convert horizontal waterline positions into vertical waterline elevations, local topographic data is required. The present work uses beach profiles from the Portuguese Environmental Agency Coastal Monitoring Program (COSMO). To ensure that the profiles covered seasonal variability, four profiles from the transect survery line in Fig.6 covering the maritime winter and summer were downloaded from COSMO's web platform for the following dates: 6th May 2021, 7th January 2021, 30th December 2019, and 30th May 2019 as shown in Fig.7.

4.1.2 Satellite Imagery

The present work used imagery from two distinct satellite missions: Sentinel-2 MSI imagery from Copernicus Mission and Planetscope imagery from Planet Mission. Table 1 presents the general characteristics of the sensors onboard each satellite mission. Planetscope and Sentinel-2 images were chosen to get high-quality sub-pixel images generated by Planetscope, as shown in Table 2, and Sentinel-2 was used for days with excessive cloud cover or missing images.

The date the beach profile survey was conducted was considered when the satellite images were downloaded. The images were downloaded based on a date interval, which spanned the period from the first to the last day of each downloaded profile month. The image extraction was limited to the profile date to prevent errors resulting from morphological changes in the profiles. A total of 51 satellite images were used in the present work, 18 from Sentinel-2 and 39 from Planetscope, covering the following months/years: December 2018, January 2019, December 2019, January 2021 and May 2021, as shown in Table 2. The dates on which the satellite images were downloaded are presented in Fig. 8.

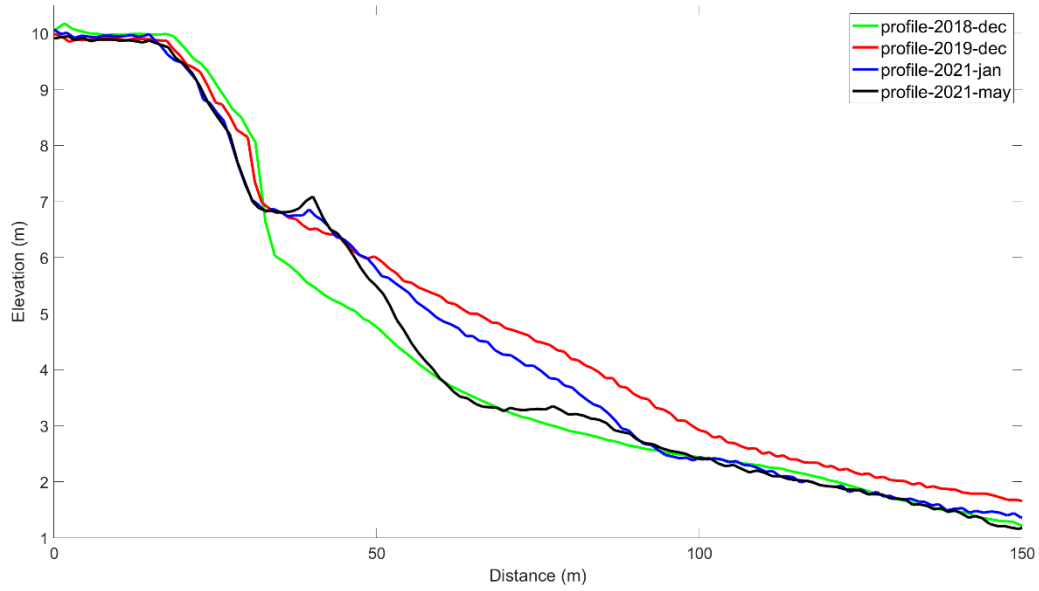

Figure 7: Profiles Downloaded from COSMOS with Distance from the Dune and Elevation. The green, red, blue, and black lines correspond to profiles downloaded in December 2018, December 2019, January 2021 and May 2021, respectively.

Table 2: Sentinel-2 and PlanetScope Image Properties

Satellite	Temporal Resolution (days)	Spatial Resolution (m)	Number of Bands	Radiometric Resolutions (bits)
Sentinel-2	5	10	13	12
PlanetScope	1	3	8	16

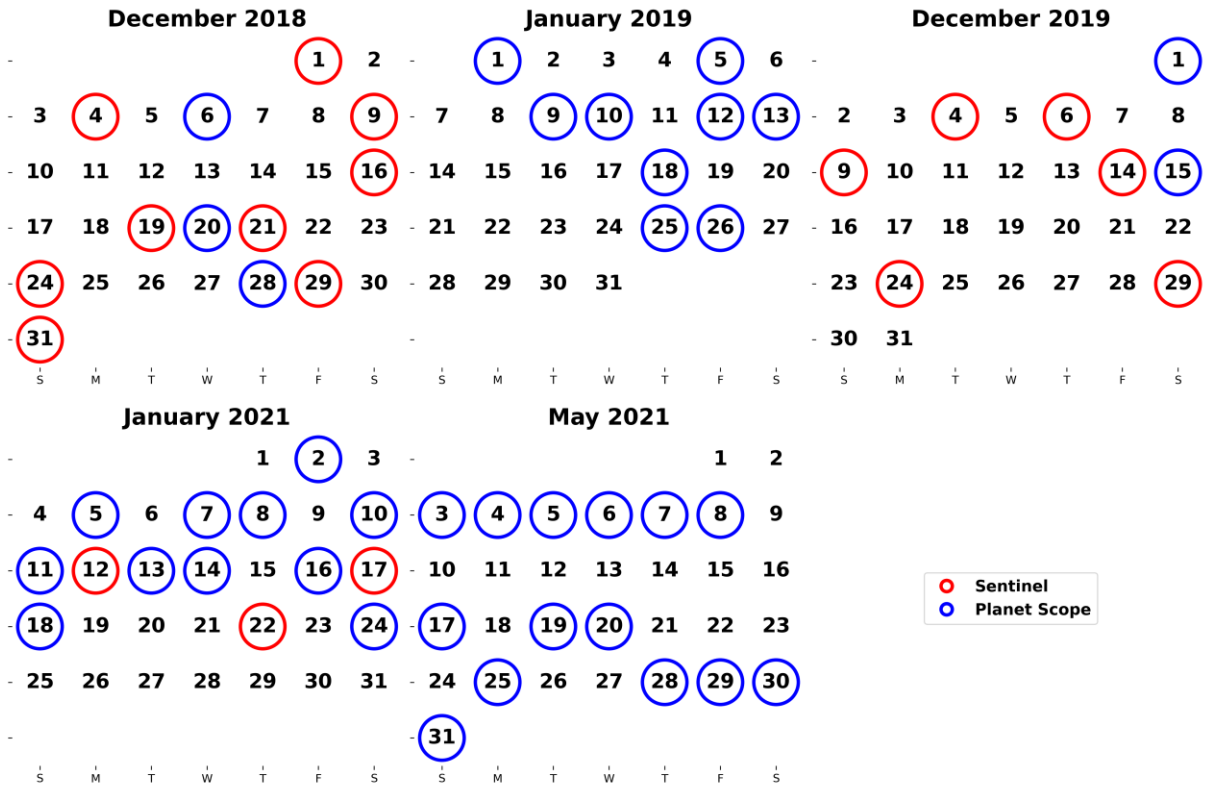

Figure 8: Calendar of the extracted satellite images, with days when images were downloaded. Days when Sentinel-2 images were downloaded are circled in red, and when Planet Scope images were downloaded are circled in Blue.

4.2 Data Processing

4.2.1 Satellite Image Horizontal Displacement Assessment

A preliminary verification of potential relative (between the images from the two distinct sensors) geometric inconsistencies was assessed. The process was done in ArcGIS using georeferencing (for image rectification), which compares the coordinates of homologous points in each image and calculates the deviations in X and Y coordinates. This was performed for a number of homologous points, and it was verified that the magnitude of the errors was sub-pixel (smaller than a meter). Therefore, it was considered that images did not require co-rectification.

4.2.2 Waterline and Wetsand Mapping

The extracted images were imported into QGIS to manually delineate the Waterline and Wetsand line, which are two of the potential runup proxies assessed in the present work. The Waterline corresponds to the instantaneous Waterline position (boundary/limit between the water and the beach) captured when the satellite sensor captures the image, while the Wetsand position (boundary between the wet and dry beach) indicates the past maximum Waterline

position reached by the highest runup levels. The Waterline was delineated based on the intersection between the maximum white patch pixel and the minimum Wetsand pixel, denoted with a deep brownish patch pixel. The Wetsand line was delineated based on the intersection between the minimum Wetsand Pixel and dry sand pixel, denoted with a lighter brownish pixel. In addition, all lines were delineated in QGIS at a scale of 1:4000 to ensure standardisation of the process. Figure 9 shows a sample of the delineated Waterline, which is red, and the Wetsand, which is blue.

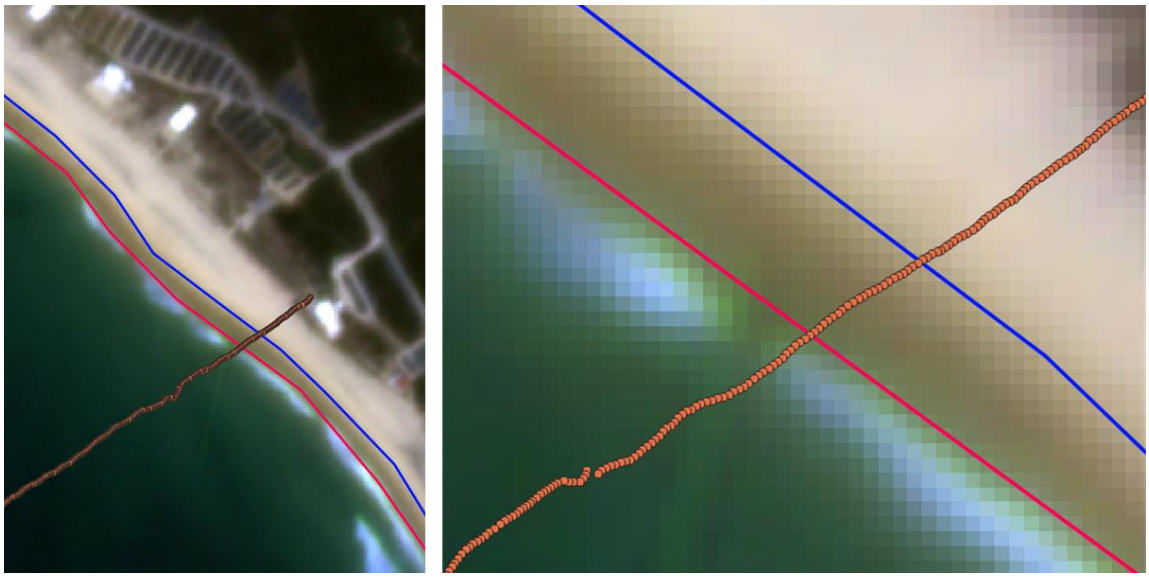

Figure 9: The Waterline and Wetsand delineation process: The Waterline is shown in red, and Wetsand in blue. The Waterline is between the minimum white and maximum brownish pixel, and Wetsand is between the minimum deep brownish pixel and the maximum less brownish pixel.

4.2.3 Converting Waterline/ Wetsand Horizontal Positions to Vertical Elevations

The horizontal extent of the satellite images' Waterline and Wetsand lines does not depict the vertical elevation. However, empirical runup formulas are based on wave-induced vertical elevation water displacements. Hence, to properly quantify the extent of the Waterline and Wetsand, the horizontal position of the delineated Waterline and Wetsand was converted to vertical height using the profile date details corresponding to that image date. As shown in Fig. 10, the profile for May 2021 was used to convert the extracted Waterline and Wetsand from an image acquired in May 2021. The procedure for converting the horizontal extent to vertical

involves getting the closest profile elevation to the Waterline and Wetsand, respectively, as shown in Figure 10.

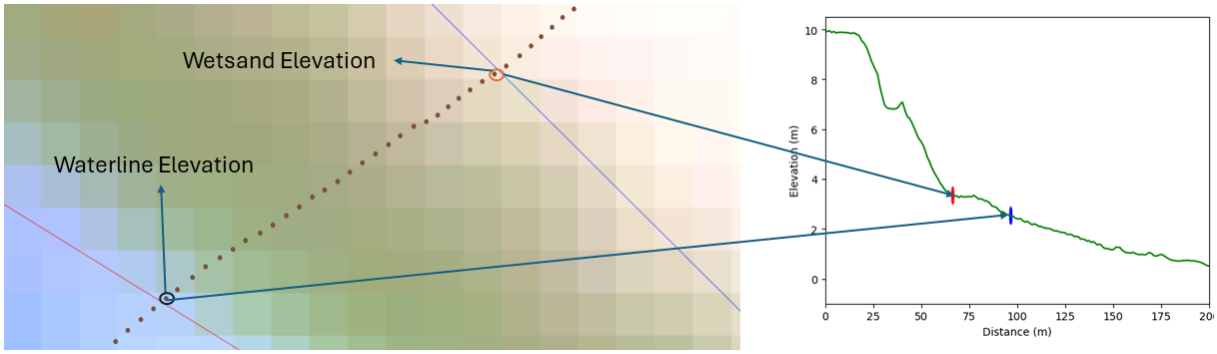

Figure 10: Waterline, Wetsand Horizontal to Vertical conversion of Image 2021-05-05 using May-05-2021 profile

4.3 Data Analysis

4.3.1 Wave and Tidal Data Exploratory Analysis

The wave and tidal data corresponding to each delineated Wetsand and Waterline parameters were merged. The process involved downloading WAVERYS wave data, a global wave reanalysis data dating from 1993. The choice of using wave data from a reanalysis model is due to the inconsistencies in the Lisbon wave buoy identified in this work. The tidal information was obtained from the FES-2014 tidal global model, an upgrade to the FES-2012 model. The FES-2014 tidal model combines the Toulouse Unstructured Grid Ocran Model (T-UGOm) and the ensemble data assimilation model, an upgrade to the FES-2012 model. The wave and tidal parameters corresponding to the satellite image acquisition time were found and used to merge hourly for each waterline and Wetsand line elevation.

4.3.2 Beach Slope Computation

As stated by previous authors, beach slope is an important parameter for estimating wave runup. Therefore, the beach slope was computed for each profile downloaded from COSMOS. The slope of the beach for each profile was computed by considering the active swash region, which is the maximum Wetsand elevation and the minimum Waterline elevation of each profile. The gradient of the swash is taken as the slope, as shown in Equation (9)

$$\frac{Ws_{\max(e)} - Wl_{\min(e)}}{Ws_{\max(d)} - Wl_{\min(d)}} \quad (9)$$

Where $Ws_{\max(e)}$ is the maximum Wetsand elevation, $Wl_{\min(e)}$ is the minimum Waterline elevation, $Ws_{\max(d)}$ is the maximum Wetsand horizontal position, and $Wl_{\min(d)}$ is the minimum waterline horizontal position respectively as shown in Figure 11.

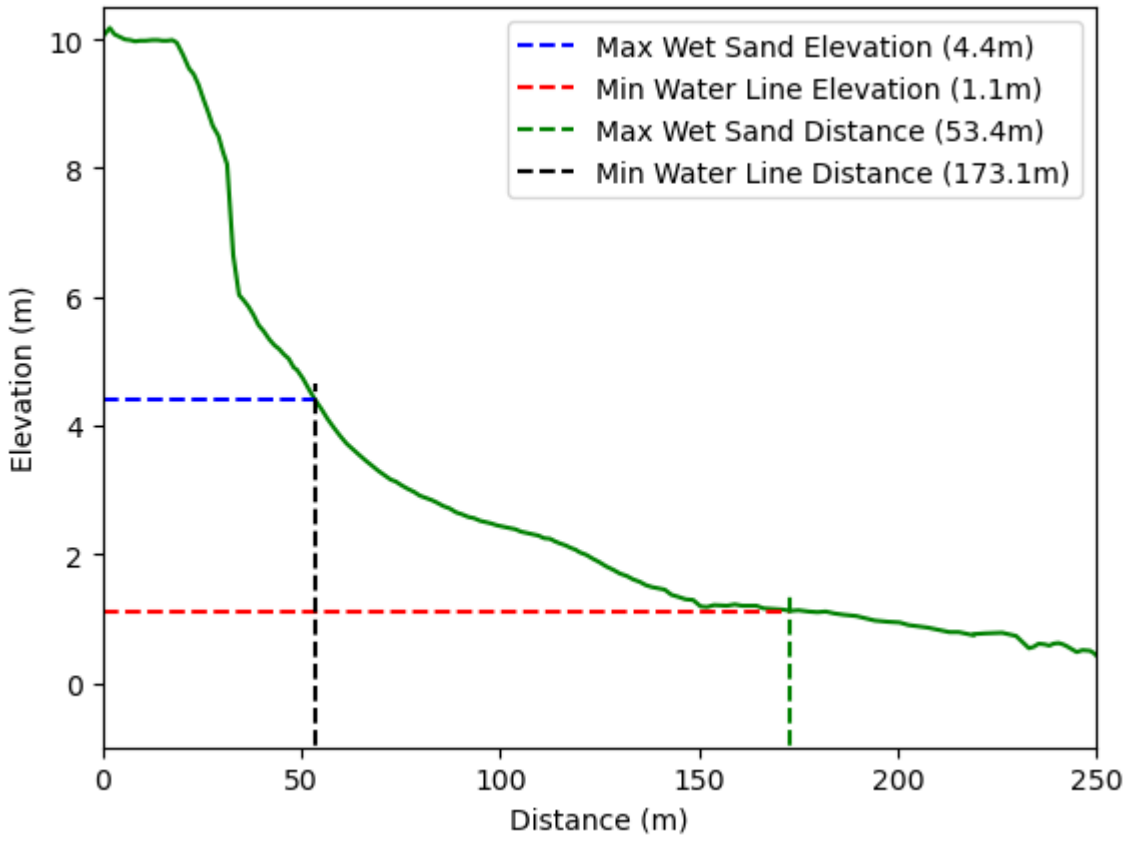

Figure 11: Beach Slope Computation: The Maximum Wetsand elevation, maximum Wetsand distance, minimum Waterline elevation, and minimum Waterline distance are shown in blue, green, red, and black, respectively.

4.3.3 Effect of Topographic Changes on Runup Proxies

In order to gain a deeper insight into the impact of beach morphology on the conversion of extracted Wetsand and Waterline horizontal extent to vertical elevation, analysis was conducted to compare the vertical elevation obtained from different profiles corresponding to each image date details with that obtained using just a single profile (2018). The impact of morphological changes and the importance of updated profiles were then studied and analysed.

5.2 Comparison of Runup Proxies with Wave Runup Formulas

The runup proxies, such as the Wetsand, Waterline, and the Average of the Waterline and Wetsand were compared to runup equations formulated by previous authors to get the most representative runup formulations. The Waterline represents the lower limit of the runup, and the Wetsand corresponds to the past runup's highest limit. Hence, the average of the Waterline and the Wetsand might capture the properties of the Waterline and the Wetsand, making it a possible runup proxy. To ensure the proxy was properly compared with the predicted runup, tidal values were added to the predicted R_2 since the proxies captured this. Hence, the R_2 referenced in the rest of the study is the predicted R_2 from past formulations plus the tidal value. The comparison methodology chosen aligns with the Gomes Da Silva et al., (2020) approach on estimating the predictive capabilities of previous runup formulations. The study chose three formulations from the selected runup formulations by Gomes Da Silva et al. (2020), which were Holman, (1986), Stockdon et al. (2006),Vousdoukas et al. (2012), as shown in Equations 10-12, respectively. The formulations were chosen based on the literature studies reviews and the coastal community's acceptance of them.

The choice of the best runup formulation for each proxy was based on the result of Root Mean Squared Error (RMSE), Bias and R-squared (R^2) between the proxy and the formulation. The equation for RMSE, Bias and R^2 are shown in Equations 13-15, respectively.

$$\frac{R_2}{H_s} = (0.83\,\xi_0 + 0.2) \tag{10}$$

$$R_2 = 1.1\left(0.35\beta_f(H_0L_0)^{\frac{1}{2}} + \frac{[H_0L_0(0.563\beta_f^2+0.004)]^{\frac{1}{2}}}{2}\right) \tag{11}$$

$$R_2 = 0.53\beta_S(H_0L_0)^{0.5} + 0.58\xi_0\sqrt{\frac{H_0^3}{L_0}} + 0.45 \tag{12}$$

$$RMSE = \sqrt{\frac{\sum_{i=1}^{N}(\text{Predicted}_i - \text{Actual}_i)^2}{N}} \tag{13}$$

Where N is the number of observations, Predicted_i corresponds to the predicted R_2 and Actual_i corresponds to the proxy of interest.

$$\text{Bias} = \frac{1}{n}\sum_{i=1}^{n}(y_i - \hat{y}_i) \tag{14}$$

Where n is the number of observations, y_i is the proxy of interest, $\hat{y}_i$ is the predicted R_2.

$$R^2 = 1 - \frac{\sum_i (y_i - \hat{y}_i)^2}{\sum_i (y_i - \bar{y})^2} \tag{15}$$

Where $\bar{y}$ is the mean of the proxy of interest

4.3.4 Satellite-derived runup formulation.

The best runup formulation for each runup proxy was chosen based on the RMSE, Bias, and R^2 results. The best runup formulations for each proxy were corrected using the Bias, and the Bias shows the difference between the proxy of interest and the predicted R_2. Hence, using the Bias value will reduce the error between the proxy and the predicted R_2.

The Bias value was added to the respective formulations, resulting in a new satellite-derived runup for each proxy.

4.3.5 Assessment of Satellite-derived runup equation during an extreme event

The corrected runup formulation for each proxy was used to predict runup during Hercule's storm, which led to overtopping at the coast of Portugal. The Hercule Storm was an extreme winter storm event between January 5th and 7th, 2014, leading to several damages (Santos et al., 2015). The maximum and minimum wave and tidal parameters corresponding to the storm events are shown in Table 3. The choice of predicting the Hercule Storm runup at the coast was to understand the performance of each proxy in predicting extreme events.

Table 3: Wave and Tide Parameters during Hercules Storm

	Hs (m)	Tp (s)	Sea Level (m ZH)
Min	2.75	13.4	0.63
Max	5.06	20.3	3.98

5.0 RESULT

5.1 Wave and Tide Parameters Analysis

Understanding the wave and tide parameters during the satellite image acquisition period is crucial. As illustrated in Figure 12, the dominant wave height observed in the images collected was less than 4 metres. Nevertheless, instances of elevated wave heights exceeding 4 m were also observed, however, they were very few. Most of the images acquired exhibited short-period waves, with a TP of less than 20 seconds, which suggests that infragravity waves did not reach the beach. The low wave height and short period may be attributed to wave breaking at the coast. The predominant wave direction is between 300 and 360 degrees, indicating that the waves originate from the north-western region, as previously observed by other authors. Despite the tidal level being below 1m for most images, the acquisition periods occurred during high tide.

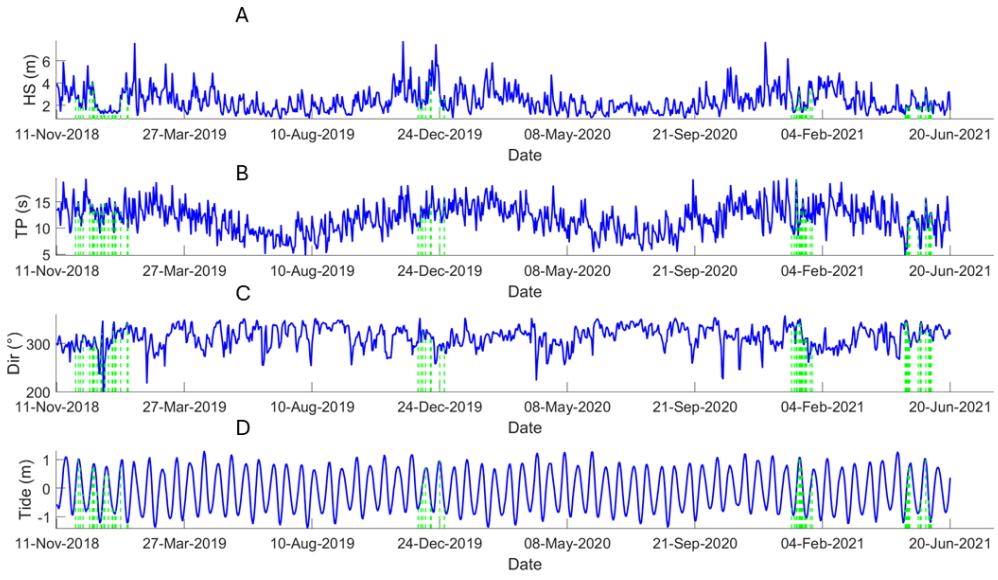

Figure 12: Timeseries plot of Wave and Tide Parameters. Subplots (A-D) are for the Wave height (HS), Peak period (TP), Wave direction and Tide level. The dashed green line indicates the image acquisition days.

5.2 Beach Morphology Effect on Runup Proxies

The impact of beach morphology while converting the runup proxies from horizontal extents to vertical elevations was investigated, and the findings are presented in Figure 13. As illustrated in Figure 13A, the wet sand vertical elevation time series obtained using just one profile (2018 profile) for all images exhibited a significant underestimation compared to those

obtained with different profiles (updated profiles). Upon examination of the highest peaks in Figure 13A, there is an approximate difference of 2m between the wet sand elevation obtained with the same and different profiles. When considering the entire time series, the Bias and RMSE between the Wetsand elevation with the same profile and different profiles are 0.72m and 0.9, respectively. A similar observation of underestimation can be noticed for the waterline elevation obtained with just one profile (2018 profile) compared to that of different profiles, as shown in Figure 13B. Furthermore, when considering the entire time series, the Bias and RMSE between the waterline elevation with the same profile and different profiles are 0.91 m and 1.122, respectively.

The distribution of the Wetsand elevation obtained with different profiles covers a wider range of elevation. In contrast, the Wetsand elevation obtained with a single profile (2018 profile) exhibits a more compact distribution, as illustrated in Figure 13C. Furthermore, there is a higher count in the elevation bins of Wetsand elevation obtained with different profiles in comparison to those obtained with the same profiles. A similar observation was made regarding the distribution of the waterline, as illustrated in Figure 13D. However, the number of counts for each elevation bin is less for the elevation obtained with different profiles than for the elevation obtained using the same profiles. Table 4 presents statistical values for the Waterline and Wetsand elevation obtained with the same profile and different profiles. The results in Figure 13 and Table 4 demonstrate that the elevation obtained with different profiles yielded a more accurate representative of the proxies than those obtained with the same profiles. Therefore, subsequent analysis should use the runup proxies obtained using different profiles.

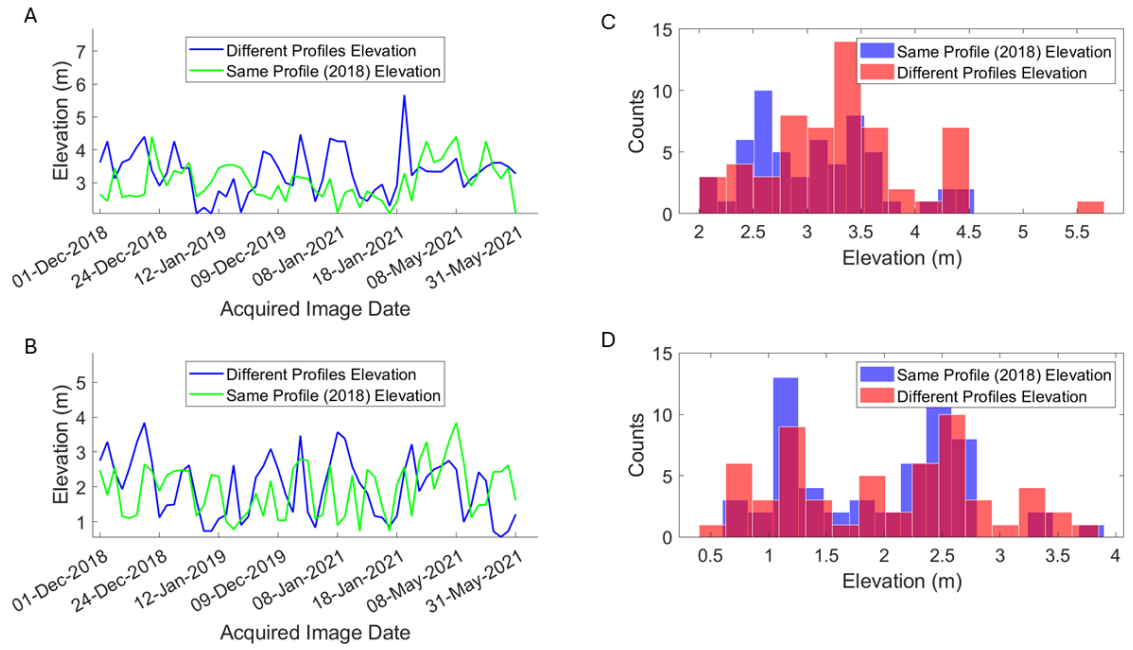

Figure 13: Effect of Beach Morphology on Runup Proxies Horizontal Extent conversion to Vertical elevation. Subplot A and B shows the time series plot between proxy elevation obtained with different profiles shown in blue and proxy elevation obtained with 2018 profile (same profile) shown in green for Wetsand and Waterline respectively. Subplot B and D shows the histogram distribution plot between proxy elevation obtained with different profiles shown in red and proxy elevation obtained with 2018 profile (same profile) shown in blue.

Table 4: Statistical metrics of Runup proxies' horizontal extent to vertical elevation for waterline and Wetsand using different profiles and same profiles (2018)

Runup Proxies	Profiles used for Elevation Conversion	Mean Elevation (m)	Median Elevation (m)	Maximum Elevation (m)	Minimum Elevation (m)	Elevation Standard Deviation
Waterline	Different	1.99	1.99	3.84	0.56	0.88
Waterline	Same (2018 profile)	1.92	2.07	3.84	0.73	0.76
Wetsand	Different	3.32	3.32	5.67	2.07	0.69
Wetsand	Same (2018 profile)	3.05	3.02	4.40	2.07	0.58

5.3 Runup Analysis

5.3.1 Comparison of Runup Equations with Runup Proxies

The runup proxies were compared with past formulations, and the findings and statistical metrics are presented in Figures 14 to 16 and Table 5. The Wetsand is more highly correlated with the predicted R_2 by Stockdon et al. (2006), as evidenced by the close alignment between the Wetsand timeseries and the predicted R_2 by Stockdon et al. (2006), as illustrated in Figure 14A. Notwithstanding, an underestimation of the Wetsand by the predicted R_2 persists in the timeseries comparison, which is indicative of errors in the prediction. The error can be observed in the high dispersion in the scatter plot between the Wetsand and the predicted R_2, as well as in the low R^2 value of 0.17, as illustrated in Figure 14C and Table 5. The predicted runup with the Holman (1986) formulation exhibited a high correlation with the Waterline proxy, as evidenced by the high level of similarity between the two timeseries and the high R^2 value of 0.63 (see Fig. 15B and Table 5). Moreover, there is a notable degree of compactness between the runup predicted by Holman and the Waterline (see Fig. 15D). Despite the high correlation and R^2, only a small number of points fall on the dashed lines, indicating a lack of perfect correlation.

The average Wetsand/Waterline exhibits a stronger correlation with the runup predicted by the Voudoukas et al. (2012) formulation, although there is an overestimation of the average Wetsand/Waterline by the predicted R_2 (see Fig 16). While the R^2 value of 0.42 is not particularly high, the scatter points exhibit a greater degree of dispersion around the best-fit line.

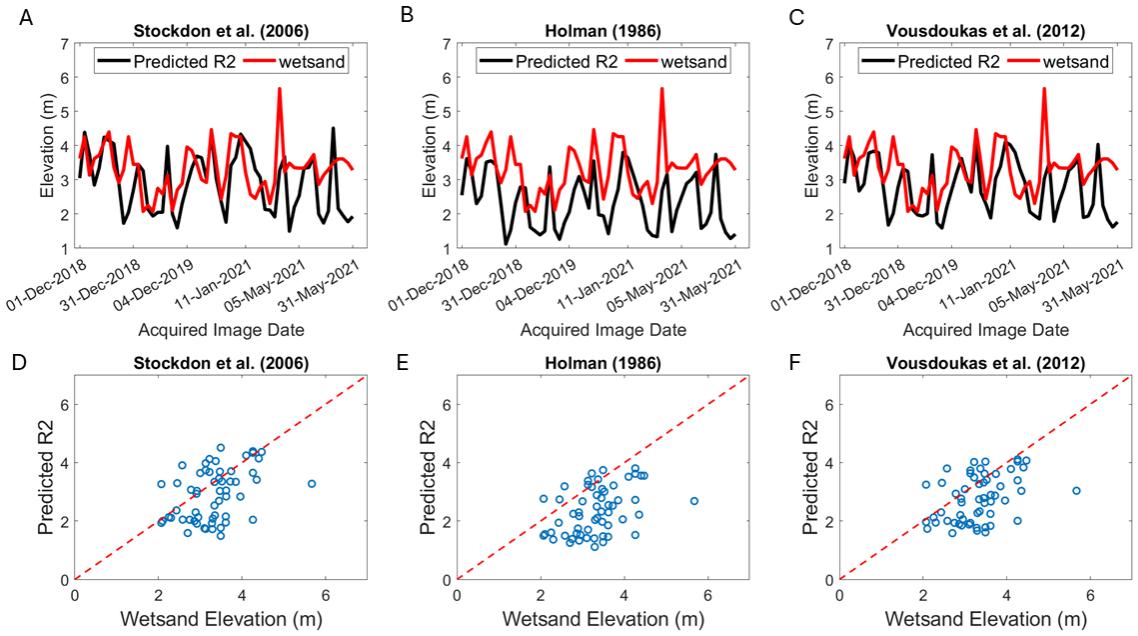

Figure 14: Wetsand Elevation comparison with runup formulations. Subplot A-C shows the timeseries comparison between Wetsand elevation and predicted R_2 for Stockdon et al. (2006), Holman (1986) and Voudouskas et al. (2012). Subplot D-F shows the scatter plot between the Wetsand elevation and predicted R_2 for Stockdon et al. (2006), Holman (1986) and Voudouskas et al. (2012).

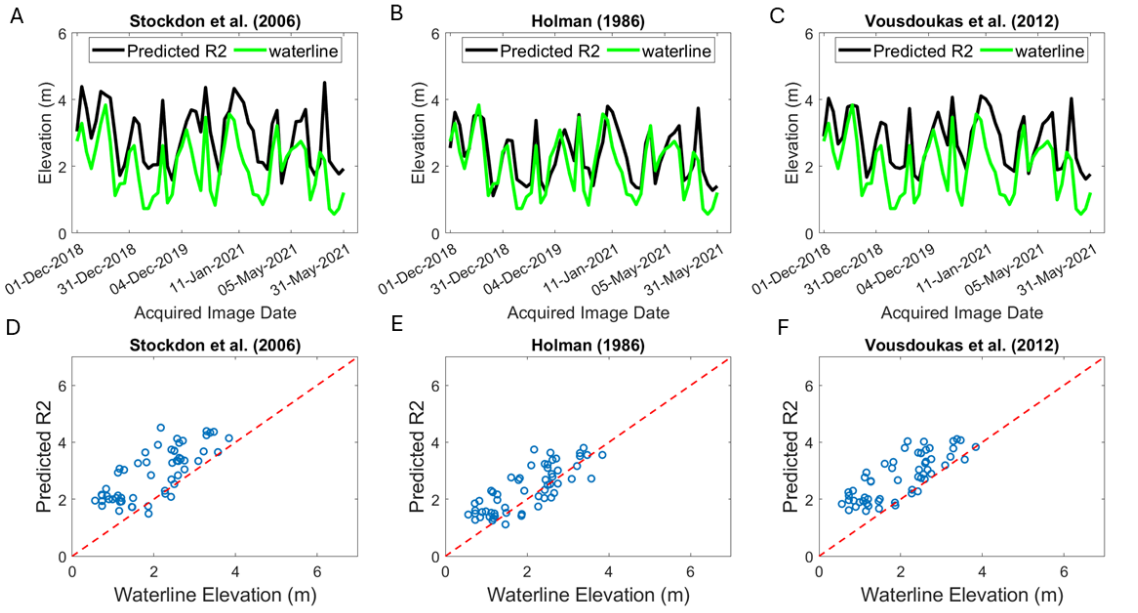

Figure 15: Waterline Elevation comparison with runup formulations. Subplot A-C shows the timeseries comparison between Waterline elevation and predicted R_2 for Stockdon et al. (2006), Holman (1986) and

Voudouskas et al. (2012). Subplot D-F shows the scatter plot between the Wetsand elevation and predicted R_2 for Stockdon et al. (2006), Holman (1986) and Voudouskas et al. (2012).

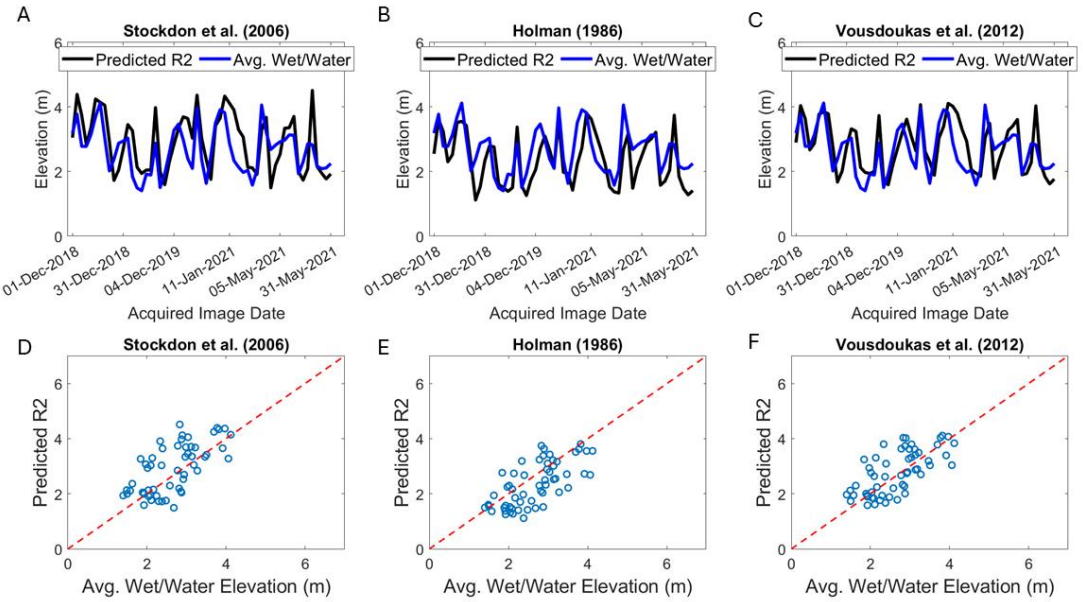

Figure 16: Average Wetsand/Waterline elevation comparison with runup formulations. Subplot A-C shows the timeseries comparison between Average Wetsand/Waterline elevation and predicted R_2 for Stockdon et al. (2006), Holman (1986) and Voudouskas et al. (2012). Subplot D-F shows the scatter plot between the Average Wetsand/Waterline elevation and the predicted R_2 for Stockdon et al. (2006), Holman (1986) and Voudouskas et al. (2012).

Table 5: Runup Proxy comparison with Runup Formulation Statistics.

Runup Formulation	Runup Proxy	Bias (m)	R^2	RMSE
R_2_Stockdon	Waterline	0.91	0.56	1.01
R_2_Holman	Waterline	0.35	0.63	0.65
R_2_Voudouskas	Waterline	0.78	0.61	0.78
R_2_Stockdon	Wetsand	-0.41	0.17	0.95
R_2_Holman	Wetsand	-0.97	0.16	1.26
R_2_Voudouskas	Wetsand	-0.54	0.16	0.97

R_2_Stockdon	Avg. Wetsand/Waterline	0.25	0.45	0.71
R_2_Holman	Avg. Wetsand/Waterline	-0.31	0.47	0.67
R_2_Voudouskas	Avg. Wetsand/Waterline	0.12	0.46	0.61

5.3.2 Choosing and correcting the best Runup Formulation for each proxy

The best runup formulation for each proxy was selected based on the Results shown in Fig. 4 and 5, as well as metrics such as R^2, RMSE, and Bias presented in Table 1. The best runup formulation for the Wetsand runup proxy is that proposed by Stockdon et al. (2006), which has an R^2 value of 0.17, an RMSE value of 0.95, and a Bias of -0.41 m, respectively. Regarding the waterline, the best formulation is Holman (1986) runup formulation, which exhibits an R^2 of 0.62, an RMSE of 0.64, and Bias of 0.35m. The best runup formulation for the Average Waterline/Wetsand is Voudouskas et al. (2012) which gave an R^2 of 0.46, an RMSE of 0.61, and Bias of 0.12m. The correction of the best formulation for each proxy was based on the Bias, which is the mean difference between each proxy and the predicted R_2. Correcting using the Bias was made because the timeseries demonstrated a difference in the vertical displacement. Therefore, a negative Bias indicates an overestimation of the expected R_2, whereas a positive Bias signifies an underestimation of the predicted R_2. Consequently, the Bias will be added to the formulation equation to correct the best formulation with a negative Bias, whereas that with a positive Bias will be subtracted from the formulation equation. The equation that has been corrected following the specified criteria for each proxy is presented below. The formulations presented in equations 16-18 represent the corrected runup equations for the Waterline, Wetsand, and average Waterline/Wetsand, as previously established by Holman (1986), Stockdon et al. (2006), and Voudouskas et al. (2012), respectively.

$$R_2 = (H_s(0.83\,\xi_0 + 0.2)) - 0.41 \quad (16)$$

$$R_2 = \left(1.1\left(0.35\beta_f(H_0L_0)^{\frac{1}{2}} + \frac{[H_0L_0(0.563\beta_f^2+0.004)]^{\frac{1}{2}}}{2}\right)\right) + 0.35 \quad (17)$$

$$R_2 = \left(0.53\beta_S(H_0L_0)^{0.5} + 0.58\xi_0\sqrt{\frac{H_0^3}{L_0}} + 0.45\right) - 0.12 \quad (18)$$

5.3.3 Assessing the Satellite-derived runup formulation for each proxy on Predicting Extreme Events

The derived satellite runup formulations were evaluated by predicting the runup associated with Hercule's storm, which resulted in overtopping at the Portuguese coast. The formulations were tested on the Maximum, Minimum values of the wave and tide parameters during the storm period (see Table 3). Table 3 shows the R_2_min and R_2_max values for the minimum and maximum wave and tide parameters during the storm conditions and for each of the best proxy formulations. Table 3 illustrates that while the waterline formulation yielded the highest R_2 for minimum wave and tide parameter values, the wet sand formulation yielded the highest R_2 under maximum wave and tide conditions.

Figure 17 illustrates the location of the highest R_2 obtained for all proxy formulations at the beach. The predicted runup for the beach profile indicates a collision rather than an overtopping (see Fig. 18). Although, the overtopping was not predicted, collision can lead to overtopping if the beach dune is weak.

Table 6: Runup Proxies formulation performance on predicting Hercule's storm Runup. R_2_min and R_2_max correspond to the runup level for the minimum and maximum wave and tide parameters during the storm period.

Proxy Formulation	R_2_min (m)	R_2_max (m)
Holman Waterline Formulation	1.53	5.34
Stockdon Wetsand Formulation	1.29	5.78
Voudouskas Average Wetsand/Waterline Formulation	1.59	5.37

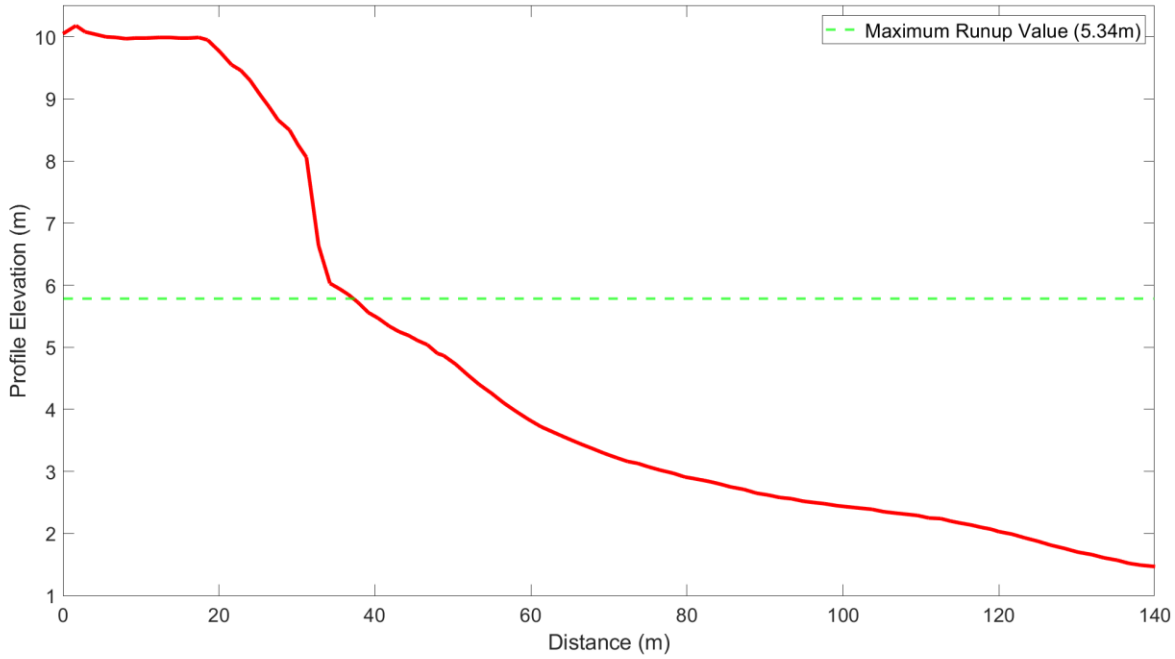

Figure 17: Assessment of the Maximum Hercule's Storm Runup Prediction Level at Costa da Caparica. The maximum runup value indicated in dashed green corresponds to the highest values of all runup proxy formulation predictions.

Figure 18: Wave collision instance at Costa da Caparica. Source

6.0 DISCUSSION

6.1 Runup Indicators

6.1.1 Wetsand and Waterline as Runup Indicators

One of the present work objectives was to investigate the use of satellite imagery to observe wave runup in a coastal sandy beach, Caparica beach. Two runup proxies, the waterline and the Wetsand lines were manually digitized from satellite images and converted into vertical heights, using local topographic data. The results demonstrated that the waterline exhibited a stronger correlation with the predicted runup, suggesting that this proxy is better related to runup processes, and may serve as a potential indicator for wave runup. In contrast, the Wetsand exhibited a comparatively weaker correlation with runup estimations. Wave parameters have been demonstrated to contribute to the extent of runup at the beach, with offshore wave height contributing to approximately 79% of the runup (Bruch et al., 2022). The existing R_2 formulations were derived based on the relationship between the wave parameters when measuring the runup and the measured runup (Holman, 1986; Stockdon et. al, 2006, Voudouskas et al. (2012). When satellite images are captured, the Waterline captures the wave-breaking process at the acquisition point. In contrast, the captured Wetsand in the image might have been produced by wave processes that occurred hours before the image acquisition. Hence, relating runup computed with the assumption that the wave parameters correspond to the time of image acquisition, will likely lead to weaker correlation which was exhibited in the Wetsand. Furthermore, the Waterline showed more correlation, because it was related to runup computed with wave parameters that corresponds to the time of acquisition. Consequently, the waterline's higher correlation coefficient than the Wetsand may be attributed to this discrepancy.

The relationship between shoreline position and wave runup was investigated by Castelle et al. (2021) through the use of satellite images to detect shoreline position. The study revealed that the extent of wave runup on the beach is significantly influenced by the shoreline position. Although the reason for the relationship was not stated, one possible reason is due to processes that determine runup extents at beaches. The extent of wave runup on the beach depends on the energy released and dissipated due to wave breaking, which occurs due to several transformations, including wave refraction, shoaling, and other coastal processes (Holman, 1986). If the shoreline position, has suffered retreat the waves will break far from the coast and the runup extent at the beach might be lower than if the shoreline position was closer to the beach. Yates et al. (2009), found a relation between the wave energy, shoreline change and the shoreline position. Hence, the position of the shoreline in relation to the tidal level during wave

breaking can be seen to determine the extent of the runup on the coast. Another potential reason why the waterline seems to outperform the wet sand is the possibility of the waterline capturing wave-breaking processes. Hence, as demonstrated in the results section, the waterline correlates more closely with the wave runup.

The difference between the predicted R_2 and the Waterline and Wetsand might be due to the lack of runup formulations capturing the effect of morphodynamics due to the beach topology and morphology, which affect wave breaking and wave runup (Stockdon et. al 2006, Holman 1986). The slope used for computing the runup, was based on the maximum Wetsand and the minimum Waterline, which underestimates the true beach slope (foreshore slope). Hence, a possible reason for the difference between the R_2 and the runup proxies. In addition, the wave parameters were obtained from a global reanalysis wave model, the wave models were obtained by forcing from global atmospheric and oceanic parameters (Fanti et al., 2023). Application of wave parameters obtained from wave models in coastal areas have proven to present errors such as overpredicting or underpredicting the wave parameters in coastal locations (Fanti et al., 2023). To overcome the errors, validation and calibration using observed wave parameters from the region of application are used. Hence, the likely reason why there are differences between the predicted R_2 using the global wave model and the proxies.

While the Waterline proved to be a better indicator based on correlations and statistical metrics, the corrected Waterline formulation only showed great performance in predicting runup when considering observed minimum wave and tide parameters during extreme events. However, the Wetsand formulation outperformed the Waterline indicator for predicting runup during extreme events with observed maximum wave and tide parameters. The underlying formulation of each proxy may explain this performance difference. The corrected Wetsand line is based on Stockdon et al. (2006), an improved version of Holman (1986) formulation on which the Waterline formulation is based. Stockdon et al. (2006) formulation was tested on several beaches, unlike Holman (1986) formulation, which was derived from a single beach. Therefore, Stockdon et al. (2006) is more generalizable and likely to yield accurate predictions. The results indicated that the Wetsand-derived runup might be a more effective predictor of R_2 in extreme events

6.1.2 Average Wetsand/ Waterline as Indicator

It has been demonstrated that Waterline and Wetsand have the potential to be used as indicators for the estimation of satellite-derived runup data. In the case of extreme maximum wave height,

it was observed that Wetsand runup indicator outperforms the Waterline runup inidcator. The potential of utilising an average between the Waterline and the Wetsand as a runup indicator was explored. The objective of averaging the Wetsand and Waterline was to combine the characteristics captured by the Wetsand with those of the waterline, to produce a more effective runup indicator.

The average Wetsand/Waterline proxy demonstrated an enhanced performance, exhibiting a reduction in mean error compared to the wetsand proxy and waterline proxy (see Table 7) However, the waterline exhibited greater performance than the average wetsand/waterline in terms of R^2, RMSE. In contrast, the average wetsand/waterline demonstrated enhanced performance compared to the wetsand in the respective metrics. In predicting extreme events, the average Wetsand/Waterline exhibited greater predictive performance than both the Waterline and the Wetsand for minimum wave and tide parameters (see Figure 19). However, the Wetsand demonstrated superior predictive performance for maximum tide and wave conditions.

Therefore, the average wetsand/waterline can be considered a reliable indicator for predicting runup when conditions are not extreme.

Table 7: Statistical Metrics comparison for the best runup proxy formulation

Runup Formulation	Runup Proxy	Bias	R^2	RMSE
R_2_holman	Waterline	0.35	0.63	0.65
R_2_stockdon	Wetsand	-0.41	0.17	0.95
R_2_Voundakatel	Average Wetsand/Waterline	0.12	0.46	1.61

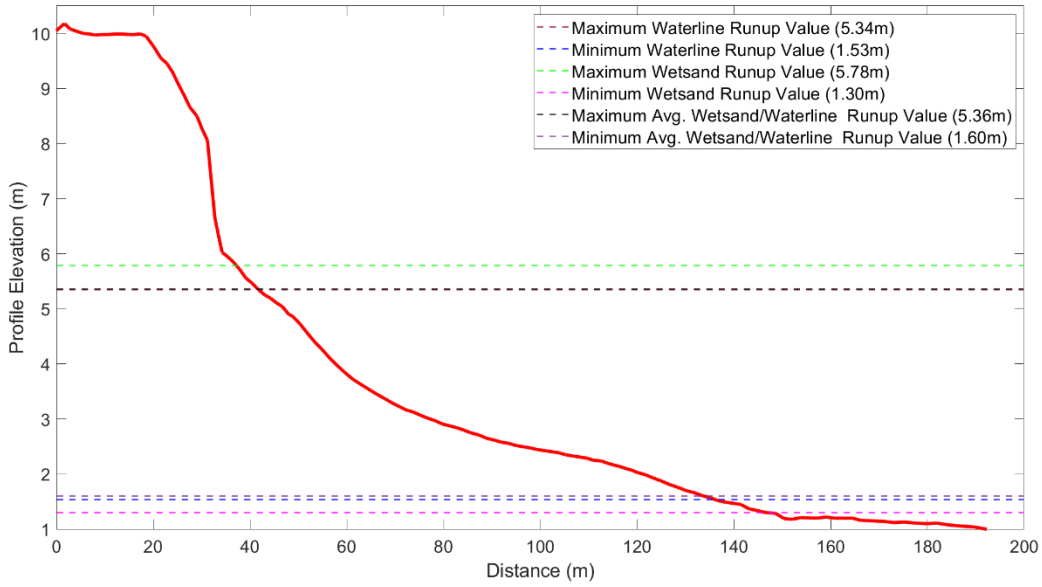

Figure 19: Hercule's storm runup prediction values for all runup proxy formulation on the beach. The beach profile corresponds to the 2018 survey profile, and the maximum and minimum values correspond to the maximum and minimum values of the wave and tide during the storm period.

6.2 Effect of Morphology/ Topography on Wave Runup

The result section demonstrates the significance of utilising an updated profile to convert the runup proxies from horizontal extent to a vertical extent. The result indicated a Bias in the magnitude of 0.72m between the Wetsand elevation converted with a single profile (2018 profile) and updated profiles. Additionally, there was approximately a 0.92m Bias (mean error) between the Waterline extracted with the same profile and that with the updated profile. Previous authors like Voundoska et al. (2012) and Stockdon et al. (2006) have employed updated profiles to convert time-stacked video images to vertical orientations. The runup obtained via video is comparable to that obtained by satellite in that both rely on the beach profile to accurately convert the horizontal extent to vertical elevation. Thus, an updated profile is necessary to convert the runup to the vertical components. The beach on Costa da Caprica is characterised by highly variable morphological and topographical features, necessitating the consideration of profile morphological changes when converting the horizontal displacements of proxies into vertical elevations.

To extend the methodology to other beaches, updated local topography must be incorporated to minimize the Bias and underestimation of runup proxies.

6.3 Application of Satellite-Derived Runup Formulations

The revised satellite-derived runup formulation was subjected to a validation process to assess its ability to predict extreme runup during the Hercules Storm. The outcomes demonstrated that the selected proxies were capable of predicting collisions for beaches. Furthermore, the corrected satellite-derived runup formulation enables runup prediction under normal conditions. It has been demonstrated that the revised satellite-derived runup formulation can capture processes previously not captured by previous runup formulations. With the advent of a revised satellite-derived formulation, the prediction of global runup is now feasible since satellite images are readily accessible.

However, for the satellite derived runup to be more effective, there needs to be a site-specific validation of the runup proxies with measured runup values corresponding to the image acquisition period. The validation will help to quantify the errors associated with the runup proxies indicators.

7.0 Conclusion / Recommendations

The objective of the study was to utilise a novel approach to estimate runup from satellite images and to identify the most relevant runup proxies from satellite images. The waterline proxy correlated with runup more with the extracted wet sand. However, the mean error metric demonstrated that the average of the waterline and wet sand proxies outperformed both the waterline and the wet sand proxies. In the context of predicting the minimum runup during extreme events, the average of the waterline and wet sand-derived runup formulations proved to be more effective, while for extreme runup events, the wet sand-derived runup formulation proved to be more accurate. The wetsand proxy exhibited a lower degree of correlation with the runup, potentially due to the captured runup being related to a previous runup instance. Although using satellite images to obtain runup data is a relatively new field of research, the potential for using satellite imagery to estimate runup has been demonstrated. Further research is needed to advance this area of study.

7.1 Challenges Faced

Some of the challenges that were faced during the study process are:

1. The limited number of profiles downloaded from COSMOS constrained the number of images that could be downloaded and, consequently, the number of proxy lines that could be extracted. The images were downloaded based on the profile date intervals. Therefore, the number of proxy lines would have been more if more profiles had been downloaded, which would have resulted in more points, thereby improving the runup formulations and increasing generality.

2. The lack of consistent wave data from Lisbon Port wave buoy, led to the use of wave data from global wave model that do not fully capture the local wave breaking wave processes. Also, the wave values generated might be over or underestimated and this might have led to errors in the computation of the R_2 and comparisons.

3. The absence of data pertaining to the captured wetsand line made it challenging to ascertain whether the wetsand line was associated with the wave and tide parameters corresponding to the time the image was acquired. This issue gave rise to the possibility of relating a different wave height to the wetsand line. In addition, it was challenging to determine whether the runup was associated with the uprush or the downrush, as depicted in the satellite images.

4. The challenge in working on the waterline was to determine whether the formation was due to a downrush or an uprush, as the satellite images did not readily identify this.

5. Unlike runup captured with videos, which have different frames of runup images, the R_2 can be easily obtained from the time stack of the frames. Satellite-captured images only contain a single image, and a time stack image cannot be formed from it, making it difficult to get the R_2 from a single image.

6. The lack of corresponding wave runup measured data, for validating and quantifying the errors associated with the satellite derived runup proxies. This was a major challenge, at properly assessing the runup proxy for Costa da Caparica.

7.2 Future Work/ Recommendations

To further make the study better and more robust, here are specific recommendations for further work and to help improve the quality of the work.

- The selection of a location with a readily available, abundant, and updated set of profiles for a specific transect will increase the number of images that can be downloaded, which in turn will facilitate the improvement of the satellite-derived runup proxies' formulation. Furthermore, if the updated profiles were created before and after a major event, this will also enhance the level of accuracy of the elevation obtained.

- Choosing a location with consistent local wave buoy data, will greatly improve the values of the wave parameters used for computing the R_2 and also better for comparing with the runup proxies.

- Acquiring satellite images with clear indication of the uprush and downrush in the image will be of help in knowing if the wetsand or waterline is related to the downrush or the uprush. At the moment, this seems not to be possible, but with advancement in satellite image acquisition, this can be possible.

- Choosing a location with corresponding field measured runup that corresponds to the date of satellite image acquisitions. Alternatively, if there are no filed measured runup values, conducting a fresh runup measurements.

- Using machine learning in addition to statistical analysis will possibly lead to an improvement in the runup formulations.

REFERENCES

Almeida, L. P., Efraim De Oliveira, I., Lyra, R., Scaranto Dazzi, R. L., Martins, V. G., & Henrique Da Fontoura Klein, A. (2021). Coastal Analyst System from Space Imagery Engine (CASSIE): Shoreline management module. *Environmental Modelling & Software*, *140*, 105033. https://doi.org/10.1016/j.envsoft.2021.105033

Bayle, P. M., Beuzen, T., Blenkinsopp, C. E., Baldock, T. E., & Turner, I. L. (2021). A new approach for scaling beach profile evolution and sediment transport rates in distorted laboratory models. *Coastal Engineering*, *163*, 103794. https://doi.org/10.1016/j.coastaleng.2020.103794

Bruch, W., Cordier, E., Floc'h, F., & Pearson, S. G. (2022). Water Level Modulation of Wave Transformation, Setup and Runup Over La Saline Fringing Reef. *Journal of Geophysical Research: Oceans*, *127*(7), e2022JC018570. https://doi.org/10.1029/2022JC018570

Cabezas-Rabadán, C., Pardo-Pascual, J. E., Palomar-Vázquez, J., Ferreira, Ó., & Costas, S. (2020). Satellite Derived Shorelines at an Exposed Meso-tidal Beach. *Journal of Coastal Research*, *95*(sp1), 1027. https://doi.org/10.2112/SI95-200.1

Costa, M., Silva, R., & Vitorino, J. (2001). *CONTRIBUTION TO THE STUDY OF THE SEA ACTIVITY CLIMATE ON THE PORTUGUESE COAST*.

Doherty, Y., Harley, M. D., Vos, K., & Splinter, K. D. (2022). A Python toolkit to monitor sandy shoreline change using high-resolution PlanetScope cubesats. *Environmental Modelling & Software*, *157*, 105512. https://doi.org/10.1016/j.envsoft.2022.105512

Fanti, V., Ferreira, Ó., Kümmerer, V., & Loureiro, C. (2023). Improved estimates of extreme wave conditions in coastal areas from calibrated global reanalyses. *Communications Earth & Environment*, *4*(1), 151. https://doi.org/10.1038/s43247-023-00819-0

Fortunato, A. B., Freire, P., Mengual, B., Bertin, X., Pinto, C., Martins, K., Guérin, T., & Azevedo, A. (2021). Sediment dynamics and morphological evolution in the Tagus Estuary inlet. *Marine Geology*, *440*, 106590. https://doi.org/10.1016/j.margeo.2021.106590

Garzon, J. L., Ferreira, A. M. M., Ferreira, Ó., Fortes, C. J., & Reis, M. T. (2020). *Beach State Report Quarteira, Praia de Faro and Costa da Caparica*.

Gomes Da Silva, P., Coco, G., Garnier, R., & Klein, A. H. F. (2020). On the prediction of runup, setup and swash on beaches. *Earth-Science Reviews*, *204*, 103148. https://doi.org/10.1016/j.earscirev.2020.103148

Holman, R. A. (1986). Extreme value statistics for wave run-up on a natural beach. *Coastal Engineering*, *9*(6), 527–544. https://doi.org/10.1016/0378-3839(86)90002-5

Holman, R. A., & Guza, R. T. (1984). Measuring run-up on a natural beach. *Coastal Engineering*, *8*(2), 129–140. https://doi.org/10.1016/0378-3839(84)90008-5

Hunt Ira A. (1959). Design of Seawalls and Breakwaters. *Journal of the Waterways and Harbors Division*, *85*(3), 123–152. https://doi.org/10.1061/JWHEAU.0000129

Longuet-Higgins, M. S., & Stewart, R. W. (1964). *Radiation stresses in Water waves; a physical discussion, with applications*.

Palma, M., Alveirinho Dias, J., & Freitas, J. G. (2021). It's not only the sea: A history of human intervention in the beach-dune ecosystem of Costa da Caparica (Portugal). *Revista de Gestão Costeira Integrada*, *21*(4), 227–247. https://doi.org/10.5894/rgci-n432

Pereira, O. N. A., Bastos, M. R., Ferreira, J. C., & Dias, J. A. (2022). Is the Sea the Enemy? Occupation and Anthropogenic Impacts at Costa da Caparica (Portugal). *Water*, *14*(18), 2886. https://doi.org/10.3390/w14182886

Ponte Lira, C., Nobre Silva, A., Taborda, R., & Freire De Andrade, C. (2016). Coastline evolution of Portuguese low-lying sandy coast in the last 50 years: An integrated approach. *Earth System Science Data*, *8*(1), 265–278. https://doi.org/10.5194/essd-8-265-2016

Raposeiro, P. D., Fortes, C. J., Capitão, R., Reis, M. T., Ferreira, J. C., Pereira, M. T. S., & Guerreiro, J. (2013). *Preliminary phases of the HIDRALERTA system: Assessment of the flood levels at S. João da Caparica beach, Portugal*. *SPEC. ISSUE 65*, 808–813. https://doi.org/10.2112/SI65-137
Sancho, F. (2023). Evaluation of Coastal Protection Strategies at Costa da Caparica (Portugal): Nourishments and Structural Interventions. *Journal of Marine Science and Engineering*, *11*(6), 1159. https://doi.org/10.3390/jmse11061159
Santos, Â., Mendes, S., & Corte-Real, J. (2015). Impacts of the storm Hercules in Portugal. *Finisterra*, vol. 49 n.º 98 (2014). https://doi.org/10.18055/FINIS6468
Silva, R., Veloso-Gomes, F., & Pais-Barbosa, J. (2013). Morphological Behaviour of Costa da Caparica Beaches Monitored during Nourishment Operations. *Journal of Coastal Research*, *165*, 1862–1867. https://doi.org/10.2112/SI65-315.1
Stockdon, H. F., Holman, R. A., Howd, P. A., & Sallenger, A. H. (2006). Empirical parameterization of setup, swash, and runup. *Coastal Engineering*, *53*(7), 573–588. https://doi.org/10.1016/j.coastaleng.2005.12.005
Synolakis, C. E. (1987). The runup of solitary waves. *Journal of Fluid Mechanics*, *185*, 523–545. https://doi.org/10.1017/S002211208700329X
Veloso-Gomes, F., Costa, J., Rodrigues, A., Taveira-Pinto, F., & Pais-Barbosa, J. (2009). Costa da Caparica Artificial Sand Nourishment and Coastal Dynamics. *Journal of Coastal Research*, *56*.
Yates, M. L., Guza, R. T., & O'Reilly, W. C. (2009). Equilibrium shoreline response: Observations and modeling. *Journal of Geophysical Research: Oceans*, *114*(C9), 2009JC005359. https://doi.org/10.1029/2009JC005359